Check for updates

RESEARCH ARTICLE

WILEY

Convergence analysis of single rate and multirate fixed stress split iterative coupling schemes in heterogeneous poroelastic media

Tameem Almani[1] | **Kundan Kumar[2]** | **Mary F. Wheeler[3]**

[1]Saudi Arabian Oil Company, Dhahran, Saudi Arabia

[2]Vista Center for Modeling of Subsurface Dynamics, Mathematics Institute, University of Bergen, Bergen, Norway

[3]Center for Subsurface Modeling, Oden Institute, UT Austin, Austin, Texas, USA

Correspondence
Tameem Almani, Saudi Arabian Oil Company, Dhahran, Saudi Arabia.
Email: tameem.almani@aramco.com

Abstract

Recently, the accurate modeling of flow-structure interactions has gained more attention and importance for both petroleum and environmental engineering applications. Of particular interest is the coupling between subsurface flow and reservoir geomechanics. Different single rate and multirate iterative and explicit coupling schemes have been proposed and analyzed in the past. In addition, Banach fixed point contraction results were obtained for iterative coupling schemes, and conditionally stable results were obtained for explicit coupling schemes. In this work, we will consider the mathematical analysis of the single rate and multirate fixed stress split iterative coupling schemes for spatially heterogeneous poroelastic media. We will re-establish the contractivity for both schemes in the localized case, and we will show that heterogeneities come at the expense of imposing more restricted conditions on the number of fine flow time steps that can be taken within one coarse mechanics time step in the multirate case. Our mathematical analysis is supplemented by numerical simulations validating our derived upper bounds. To the best of our knowledge, this is the first rigorous mathematical analysis of the multirate fixed-stress split iterative coupling scheme in heterogeneous poroelastic media.

KEYWORDS

fixed-stress split iterative coupling, heterogeneous poroelastic media, contraction mapping, poroelasticity

1 | INTRODUCTION

Currently, the coupling between subsurface flow and reservoir geomechanics is an active area of research. In fact, a clear understanding of the fluid flow and the solid-phase mechanical response is needed for the accurate modeling of multiscale and multiphysics phenomena such as reservoir deformation, surface subsidence, well stability, sand production, waste deposition, pore collapse, fault activation, hydraulic fracturing, CO_2 sequestration, and hydrocarbon recovery [30, 40]. Traditionally, the main purpose of performing reservoir simulation was to obtain accurate results for reservoir flow in which the effects of porous media deformations are approximated by a constant rock compressibility factor. In fact, such mechanical deformations have a direct impact on the pore pressure which, in turn, affects the accuracy of reservoir flow models [40]. By oversimplifying the rock compressibility coefficient with a constant rock compressibility term, the solid phase stress and strain can never be accounted for. This poses several concerns on the accuracy of flow models in stress-sensitive and naturally fractured reservoirs [40]. Therefore, it is only through the accurate coupling between subsurface flow and reservoir geomechanics that accurate and trusted results can be deduced from flow models in such types of reservoirs.

The coupled flow and geomechanics problem has been heavily investigated in the past. The seed of this work can be tracked down to the work of Terzaghi [54] and Biot [9, 10]. Terzaghi was the first to propose an explanation of the soil consolidation process. He analyzed the settlement of a column of soil under a constant load which is prevented from lateral expansion. The success of Terzaghi's theory in predicting the settlement of different types of soils led to the creation of the science of soil mechanics [10]. More details about Terzaghi's theory of consolidation can be found in [54]. Terzaghi's one dimensional work was then extended by Biot to the three-dimensional case [10]. Several studies and interpretations based on Biot's consolidation theory can be found in [28, 46]. To name just a few, Geertsma [28] utilized Biot theory to present a unified treatment of rock mechanics problems in the field of petroleum production engineering. Rice and Cleary [46] considered applications of the Biot linearized quasi-static elasticity theory of fluid-saturated porous media. Coussy [21] presented the general theory of thermoporoelastoplasticity for saturated materials. Other nonlinear extensions of the theory of poroelasticity can be found in [19, 20, 24, 26, 49, 52].

Several approaches to decompose and reformulate coupled multiphysics problems into simpler subproblems exist in literature. For example, at the continuum mechanics level, iterative domain decomposition methods, such as the Schwarz alternating method, have been developed to enable continuum-to-continuum coupling in dynamic and quasistatic solid mechanics domains respectively [32, 42, 43]. Such methods consider solving the mechanics problem in two different domains through a coupling interface whereas in our approach, we solve two different physical problems at the same domain. An alternative approach to decomposition of a multiphysics problem is the work of [11] which employs PDE-constrained optimization techniques to break down the coupled problem into a sequence of component physics problems that can be solved more robustly and efficiently using legacy codes for each component physics problem separately. For each subproblem, a suitable objective functional and a set of control variables are chosen such that the subproblem can be reformulated as a minimization problem subject to the constraints provided by the corresponding component physics subproblem. This is a variation of the works of [38, 39] that employ an optimization based strategy using virtual controls for the decomposition of the domain, the operators, and the energy spaces as well. In their approach, the virtual controls correspond to the solution of the underlying PDE, and the constraints are the copies of the original PDE. In contrast, we will consider a physics-based splitting of our coupled problem on a single computational domain.

There are three major approaches of coupling fluid flow with reservoir mechanics, known as the fully implicit, the explicit, and the iterative coupling schemes. The fully implicit scheme solves the two problems simultaneously and a preconditioning technique can be employed to decouple the two problems at the linear solver level [18, 25]. In contrast, the explicit coupling scheme decouples the two problems, and solves them in a sequential manner [2, 4]. The iterative coupling scheme lies in between these two approaches, decouples the two problems, and imposes an iteration between the two until convergence is obtained [3, 5–7, 36].

Four major iterative coupling schemes for coupling flow with geomechanics exist in literature, known as the fixed-stress, fixed-strain, drained, and undrained split iterative coupling schemes. For a variational characterization of these schemes, we refer to the recent work [16]. Out of these four methods, the fixed stress split and the undrained split schemes were shown to be convergent, while the fixed strain split and the drained split schemes were shown to be only conditionally stable [33–35, 41]. This led to a huge emphasis on studying and extending the fixed stress split and the undrained split schemes in contrast to the fixed strain and the drained split schemes. For example, a parallel in time extension of the fixed stress split scheme was proposed in the work of [12], and a fixed-stress split based preconditioner for the the simultaneously coupled system was proposed in the work of [18, 26, 27, 57]. There has been an investigation into the optimization of fixed stress algorithm in [53]. Multiphase flow coupled with linear/nonlinear geomechanics has been solved using iterative algorithm and its variants [15, 44, 45]. Moreover, we refer the reader to [31] for iterative algorithms applied to an extension of Biot model that includes multiple pressure fields with biological applications. Furthermore, a priori error estimates and a posteriori error estimates of these iterative algorithms have been studied and developed in [1, 29, 37].

The coupled flow and geomechanics problem induces two characteristic time scales, one for mechanics and the other for flow. These time scales may be different and we can exploit this fact to design the so-called multirate schemes. In these schemes, we take different time steps for the flow and for the mechanics. Assuming the mechanics time step to be slower in general, as is typically the case in subsurface dynamics, we can take several fine flow time steps for each coarse mechanics time step. The existing splitting schemes provide a natural way to consider the multirate scheme as the two equations are decoupled. This allows us to choose appropriate time steps for each equation separately. Similarly, we can also consider independent discretizations for the mechanics and flow equations giving rise to multiscale approaches [22]. Multirate extensions of the undrained split and the fixed stress split schemes were proposed in the work of [3, 36], and nonlinear and multiscale extensions of the fixed stress split scheme were proposed in the work of [13] and [22, 23]. Moreover, the convergence of the undrained split iterative scheme in heterogenous poroelastic media was established in the work of [8] for both the single rate and multirate schemes, and the convergence of the single rate fixed stress split scheme in heterogeneous poroelastic media was addressed in the work of [14]. At this stage, it is worth mentioning that the multirate approach is motivated from the field of solving ordinary differential equations [48]. In other multiphysics applications, for example, involving Stokes Darcy type or other hyperbolic models, multirate approaches have been used in [17, 47, 50]. In this article, we will follow an approach similar to the one presented in [8] to establish the convergence of the single rate and multirate fixed stress split scheme in heterogenous poroelastic media.

As stated above, by extending the work of [3] to include heterogeneities in the poroelastic parameters, we will establish fixed point Banach contraction for both the single rate and multirate fixed stress iterative coupling schemes in heterogeneous poroelastic media. Figure 1a,b show the difference between the single rate and multirate coupling schemes. In the single rate case, the flow and mechanics problems share the same time step, while in the multirate scheme the flow takes multiple finer time steps within one coarse mechanics time step. It should be noted here that for the multirate scheme,
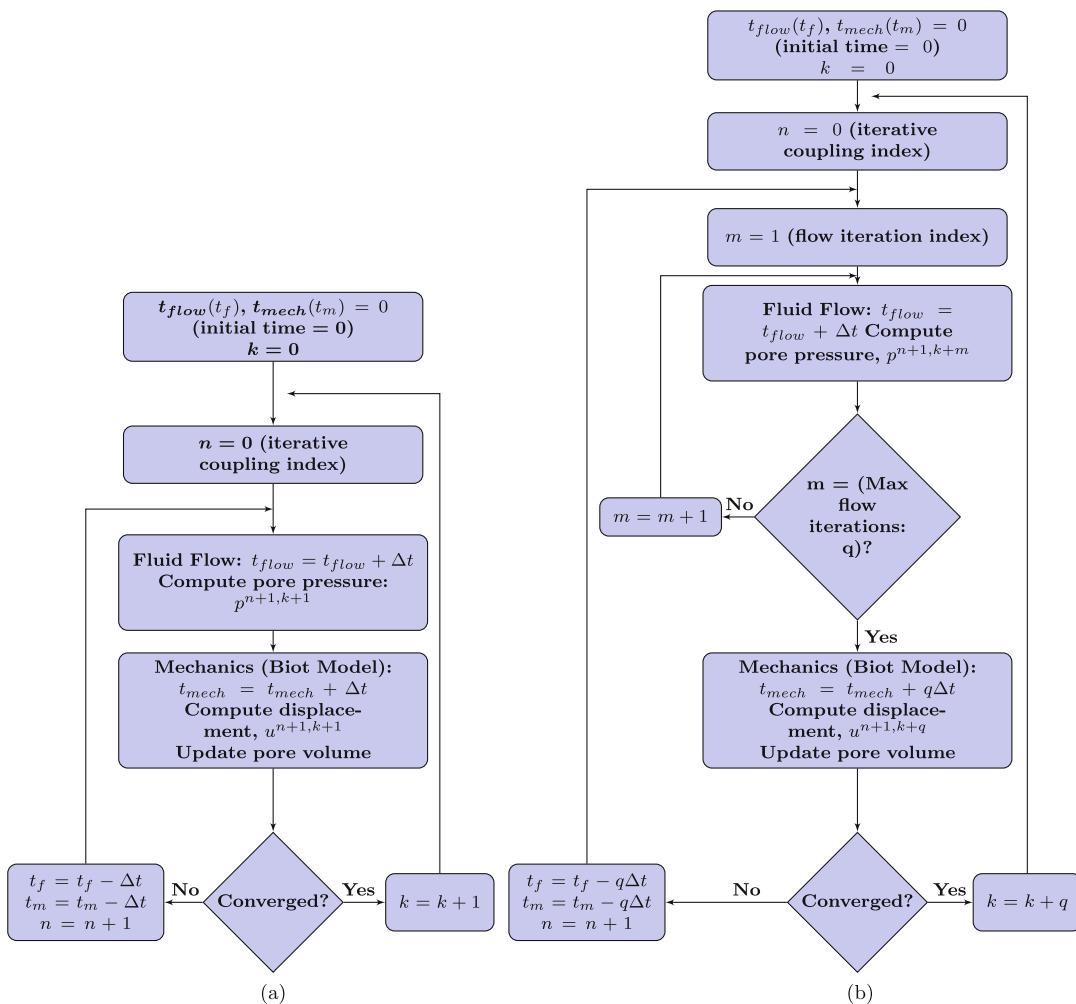
FIGURE 1 Flowchart for the iterative coupling algorithm using single rate and multirate time stepping for coupled geomechanics and flow problems. (a) Single rate; (b) multirate.

heterogeneities in the poroelastic parameters come at the expense of imposing an upper bound on the number of flow fine time steps solved within one coarse mechanics time step. In addition, our localized proof outlines a general strategy that is very likely to be useful for obtaining similar localized estimates for other iterative and explicit coupling schemes.

The article is structured as follows. Model equations and associated discretizations are presented in Section 2. Sections 3 and 4 present the formulations and analyses for the localized single rate and multirate iterative coupling schemes respectively. Section 4 compares multirate Banach contraction results established for homogeneous versus heterogeneous poroelastic media. Numerical results for a realistic reservoir model, with a heterogeneous permeability distribution, are shown in Section 6. Conclusions and outlook are discussed in Section 7.

1.1 | Preliminaries

Let Ω be an open, connected, and bounded domain of $\mathbb{R}^d$, where the dimension $d = 2$ or 3, with a Lipschitz continuous boundary $\partial\Omega$. For the pressure unknown, we assume that the boundary is

decomposed into Dirichlet boundary Γ_D, and Neumann boundary Γ_N, associated with Dirichlet and Neumann boundary conditions respectively, such that $\Gamma_D \cup \Gamma_N = \partial\Omega$. In addition, let $\mathfrak{D}(\Omega)$ be the space of all functions that are infinitely differentiable and with compact support in Ω, and let $\mathfrak{D}'(\Omega)$ be its dual space, that is, the space of distributions in Ω. As usual, we denote by $H^1(\Omega)$ the classical Sobolev space

$$H^1(\Omega) = \left\{ v \in L^2(\Omega); \nabla v \in L^2(\Omega)^d \right\},$$

equipped with the semi-norm and norm:

$$|v|_{H^1(\Omega)} = \|\nabla v\|_{L^2(\Omega)^d}, \qquad \|v\|_{H^1(\Omega)} = \left(\|v\|_{L^2(\Omega)}^2 + |v|_{H^1(\Omega)}^2 \right)^{1/2}.$$

More generally, for $1 \le p < \infty$, $W^{1,p}(\Omega)$ is the space

$$W^{1,p}(\Omega) = \left\{ v \in L^p(\Omega); \nabla v \in L^p(\Omega)^d \right\},$$

normed by

$$|v|_{W^{1,p}(\Omega)} = \|\nabla v\|_{L^p(\Omega)^d}, \qquad \|v\|_{W^{1,p}(\Omega)} = \left(\|v\|_{L^p(\Omega)}^p + |v|_{W^{1,p}(\Omega)}^p \right)^{1/p},$$

with the standard modification for the case when $p = \infty$. We also define:

$$H_0^1(\Omega) = \left\{ v \in H^1(\Omega); v|_{\partial\Omega} = 0 \right\},$$

and for the divergence operator, we shall use the spaces

$$H(\mathrm{div};\Omega) = \left\{ \mathbf{v} \in L^2(\Omega)^d; \nabla \cdot \mathbf{v} \in L^2(\Omega) \right\},$$

and

$$H_0(\mathrm{div};\Omega) = \left\{ \mathbf{v} \in H(\mathrm{div};\Omega)^d; \mathbf{v} \cdot \mathbf{n} = 0 \ \ \text{on} \ \ \partial\Omega \right\},$$

equipped with the norm

$$\|\mathbf{v}\|_{H(\mathrm{div};\Omega)} = \left(\|\mathbf{v}\|_{L^2(\Omega)^d}^2 + \|\nabla \cdot \mathbf{v}\|_{L^2(\Omega)}^2 \right)^{1/2}.$$

We recall the definition of the symmetric strain tensor: $\boldsymbol{\varepsilon}(v) = \frac{1}{2} \left(\nabla v + (\nabla v)^T \right)$, for a vector v in $\mathbb{R}^d$. For completeness, we list below two useful inequalities that will be used:

- Poincaré's inequality in $H_0^1(\Omega)$:

There exists a constant $\mathcal{P}_\Omega$ depending only on Ω such that

$$\forall v \in H_0^1(\Omega), \|v\|_{L^2(\Omega)} \le \mathcal{P}_\Omega |v|_{H^1(\Omega)}. \tag{1}$$

- Korn's first inequality in $H_0^1(\Omega)^d$:

There exists a constant C_κ depending only on Ω such that

$$\forall \mathbf{v} \in H_0^1(\Omega)^d, |\mathbf{v}|_{H^1(\Omega)^d} \le C_\kappa \|\boldsymbol{\varepsilon}(\mathbf{v})\|_{L^2(\Omega)^{d\times d}}. \tag{2}$$

2 | MODEL EQUATIONS AND DISCRETIZATION

We assume a linear and elastic porous medium $\Omega \subset \mathbb{R}^d$, $d = 2$ or 3, in which the reservoir is saturated with a slightly compressible fluid. We start by describing the geomechanics model, followed by the flow model.

2.1 | Geomechanics model

Using a quasi-static (i.e., ignoring the second order time derivative for the displacement) Biot approach to obtain the displacements (see [10]), the "geomechanics" model is as follows:

$$\sigma^{\mathrm{por}}(\boldsymbol{u}, p) = \sigma(\boldsymbol{u}) - \alpha\, p \boldsymbol{I}, \tag{3}$$

$$\sigma(\boldsymbol{u}) = \lambda(\nabla \cdot \boldsymbol{u})\boldsymbol{I} + 2\, G\varepsilon(\boldsymbol{u}), \tag{4}$$

$$-\mathrm{div}\,\sigma^{\mathrm{por}}(\boldsymbol{u}, p) = \boldsymbol{f} \qquad \text{in } \Omega, \tag{5}$$

where σ^{por} is the Cauchy stress tensor, $\boldsymbol{I}$ is the identity tensor, $\boldsymbol{u}$ is the solid's displacement, p is the fluid pressure, $\alpha > 0$ is the dimensionless Biot coefficient, σ is the effective linear elastic stress tensor, $\lambda > 0$ and $G > 0$ are the Lamé constants, $\boldsymbol{f}$ is a body force, which is usually assumed to be a gravity loading term. The last equation represents the balance of linear momentum in the solid.

2.2 | Single phase flow model

Following a slightly different formulation compared to the one described in [30], we assume a linearized slightly compressible single-phase flow model for the fluid in the reservoir. As listed in the assumptions above, we also assume that $\boldsymbol{K}$, the absolute permeability tensor, is bounded, symmetric, and uniformly positive definite in space and constant in time (for discrete time intervals). The fluid density, ρ_f is assumed to be a linear function of pressure: $\rho_f = \rho_{f,r}\,(1 + c_f(p - p_r))$. The porosity, or the fluid content of the medium, denoted by φ^* is related to the "mechanical" displacement and "fluid" pressure by this relation: $\varphi^* = \varphi_0 + \alpha\nabla \cdot \boldsymbol{u} + \frac{1}{M}p$, where φ_0 is the initial porosity, and M is the Biot constant. The fluid mass balance in the reservoir, denoted by Ω, reads: $\frac{\partial}{\partial t}\left(\rho_f \varphi^*\right) + \nabla \cdot \left(\rho_f \boldsymbol{v}^D\right) = q_s$, where q_s is a mass source or sink term, and $\boldsymbol{v}^D$ is the velocity of the fluid in Ω, $\boldsymbol{v}^D = -\frac{1}{\mu_f}\boldsymbol{K}\left(\nabla p - \rho_f g\nabla\eta\right)$. Substituting the definitions of $\boldsymbol{v}^D$, ρ_f, and φ^* into the mass balance equation, we get:

$$\frac{\partial}{\partial t}\left(\rho_{f,r}\left(1 + c_f\left(p - p_r\right)\right)\left(\varphi_0 + \alpha\nabla \cdot \boldsymbol{u} + \frac{1}{M}p\right)\right) + \nabla \cdot \left(\rho_{f,r}\left(1 + c_f\left(p - p_r\right)\right)\boldsymbol{v}^D\right) = q_s.$$

which can be written as (after re-arranging terms):

$$\rho_{f,r}\left(\frac{1}{M}\left(1 + c_f\left(p - p_r\right)\right) + c_f\left(\varphi_0 + \alpha\nabla \cdot \boldsymbol{u} + \frac{1}{M}p\right)\right)\frac{\partial}{\partial t}p + \rho_{f,r}\alpha\left(1 + c_f\left(p - p_r\right)\right)\nabla \cdot \frac{\partial}{\partial t}\boldsymbol{u}$$
$$+ \nabla \cdot \left(\rho_{f,r}\left(1 + c_f\left(p - p_r\right)\right)\boldsymbol{v}^D\right) = q_s.$$

For the sake of linearization, we assume that the fluid compressibility c_f is small, in the order of 10^{-5} or 10^{-6}, and the term $c_f(p - p_r)$ is also small as well (of the same order). We make the following approximations: $\frac{1}{M}\left(1 + c_f\left(p - p_r\right)\right) \approx \frac{1}{M}$, $c_f\left(\varphi_0 + \alpha\nabla \cdot \boldsymbol{u} + \frac{1}{M}p\right) \approx c_f\varphi_0$, $\rho_{f,r}(1 + c_f(p - p_r))\alpha \approx \rho_{f,r}\alpha$, $\rho_{f,r}(1 + c_f(p - p_r))\boldsymbol{v}^D \approx \rho_{f,r}\boldsymbol{v}^D$, $\rho_{f,r}(1 + c_f(p - p_r))g\nabla\eta \approx \rho_{f,r}g\nabla\eta$. With such approximations, the mass balance equation now reads:

$$\rho_{f,r}\left(\frac{1}{M} + c_f\varphi_0\right)\frac{\partial}{\partial t}p + \rho_{f,r}\alpha\nabla \cdot \frac{\partial}{\partial t}\boldsymbol{u} + \rho_{f,r}\nabla \cdot \boldsymbol{v}^D = q_s$$

which can be written as (after dividing by $\rho_{f,r}$, and submitting the expression of $\boldsymbol{v}^D$):

$$\frac{\partial}{\partial t}\left(\left(\frac{1}{M} + c_f\varphi_0\right)p + \alpha\nabla \cdot \boldsymbol{u}\right) - \nabla \cdot \left(\frac{1}{\mu_f}\boldsymbol{K}\left(\nabla p - \rho_{f,r}g\nabla\eta\right)\right) = \widetilde{q}, \tag{6}$$

where $\widetilde{q} = \frac{q_s}{\rho_{f,r}}$. This completes the derivation of the poro-elastic equations, modeling the displacement $\boldsymbol{u}$ and pressure p in Ω.

Therefore, our quasi-static Biot model, which is quite standard in literature [10, 30], reads: Find $\boldsymbol{u}$ and p satisfying the equations below for all time $t \in]0, T[$:

$$-\operatorname{div}\boldsymbol{\sigma}^{\mathrm{por}}(\boldsymbol{u}, p) = \boldsymbol{f} \text{ in } \Omega,$$

$$\boldsymbol{\sigma}^{\mathrm{por}}(\boldsymbol{u}, p) = \boldsymbol{\sigma}(\boldsymbol{u}) - \alpha p \boldsymbol{I} \text{ in } \Omega,$$

$$\boldsymbol{\sigma}(\boldsymbol{u}) = \lambda(\nabla \cdot \boldsymbol{u})\boldsymbol{I} + 2G\boldsymbol{\varepsilon}(\boldsymbol{u}) \text{ in } \Omega,$$

$$\frac{\partial}{\partial t}\left(\left(\frac{1}{M} + c_f\varphi_0\right)p + \alpha\nabla \cdot \boldsymbol{u}\right) - \nabla \cdot \left(\frac{1}{\mu_f}\boldsymbol{K}\left(\nabla p - \rho_{f,r}g\nabla\eta\right)\right) = \widetilde{q} \text{ in } \Omega,$$

Boundary conditions: $\boldsymbol{u} = \boldsymbol{0}$ on $\partial\Omega$, $\boldsymbol{K}\left(\nabla p - \rho_{f,r}g\nabla\eta\right)\cdot\boldsymbol{n} = 0$ on Γ_N, $p = 0$ on Γ_D,

Initial condition $(t = 0):$ $\left(\left(\frac{1}{M} + c_f\varphi_0\right)p + \alpha\nabla \cdot \boldsymbol{u}\right)(0) = \left(\frac{1}{M} + c_f\varphi_0\right)p_0 + \alpha\nabla \cdot \boldsymbol{u}_0,$

where: g is the gravitational constant, η is the distance in the vertical direction (assumed to be constant in time), $\rho_{f,r} > 0$ is a constant reference density (relative to the reference pressure p_r), φ_0 is the initial porosity, M is the Biot constant, $\widetilde{q} = \frac{q_s}{\rho_{f,r}}$ where q_s is a mass source or sink term taking into account injection into or out of the reservoir. We remark that the first three equations describe the mechanics whereas the fourth one is the flow equation. Note that the above system is linear and coupled.

2.3 | Mixed variational formulation

A mixed formulation will be used for the flow equations and conformal Galerkin will be used for the mechanics equation. In the mixed method, the flux is defined as a separate unknown, and the flow equation is rewritten as a system of first order equations. This formulation is a standard one for flow equations as it is locally mass conservative and computes the flux explicitly. For time discretization, we will assume a backward-Euler scheme (for both the continuous and discrete in space formulations).

Accordingly, for the fully discrete formulation (discrete in time and space), let $\mathfrak{T}_h$ denote a regular family of conforming triangular elements of the domain of interest, $\overline{\Omega}$. Using the lowest order Raviart–Thomas (RT) spaces, we have the following discrete spaces ($\boldsymbol{V}_h$ for discrete displacements, Q_h for discrete pressures, and $\boldsymbol{Z}_h$ for discrete velocities (fluxes)):

$$\boldsymbol{V}_h = \left\{\boldsymbol{v}_h \in H^1(\Omega)^d; \forall T \in \mathfrak{T}_h, \boldsymbol{v}_{h|T} \in \mathbb{P}_1^d, \boldsymbol{v}_{h|\partial\Omega} = \boldsymbol{0}\right\} \tag{7}$$

$$Q_h = \left\{p_h \in L^2(\Omega); \forall T \in \mathfrak{T}_h, p_{h|T} \in \mathbb{P}_0\right\} \tag{8}$$

$$\boldsymbol{Z}_h = \left\{\boldsymbol{q}_h \in H(\operatorname{div}; \Omega); \forall T \in \mathfrak{T}_h, \boldsymbol{q}_{h|T} \in \mathbb{P}_1^d, \boldsymbol{q}_h \cdot \boldsymbol{n} = 0 \text{ on } \Gamma_N\right\} \tag{9}$$

The space of displacements, $\boldsymbol{V}_h$, is equipped with the norm:

$$\|\boldsymbol{v}\|_{V_h} = \left(\sum_{i=1}^d \|v_i\|_{H^1(\Omega)}^2\right)^{1/2}.$$

We also assume that the finer time step is given by: $\Delta t_k = t_k - t_{k-1}$. In this work, we assume uniform fine flow time steps, so for simplicity, we will drop the subscript k, and denote the fine time step by Δt. If we denote the total number of timesteps by N, then the total simulation time is given by $T = \Delta t$ N, and $t_i = i\Delta t$, $0 \leqslant i \leqslant N$ denote the discrete time points.

For the fully discrete scheme, we have chosen the RT spaces for the mixed finite element discretization. However, the proof extends to other choices for the mixed spaces (e.g., the multipoint flux mixed finite element spaces [55, 56]).

> *Remark* 1 **Notation:** Two indices will be used in this article, one for the time step and the other for the coupling between the mechanics and flow. The following notations will be employed, n denotes the coupling iteration index, k denotes the coarser (mechanics) time step iteration index, m denotes the finer (flow) time step iteration index, Δt stands for the time step, and q is the "fixed" number of local flow time steps per coarse mechanics time step. A schematic showing the relations between k, m, q, and Δt can be found in Figure 1b. In addition, for a given time step $t = t_k$, we define the difference between two coupling iterates as:
>
> $$\delta\xi^{n+1,k} = \xi^{n+1,k} - \xi^{n,k},$$
>
> where ξ may stand for p_h, z_h, or $\boldsymbol{u}_h$ (the discrete pressure, flux, and displacements variables).

2.4 | Assumptions

We have the following assumptions on the model and data:

1. For mechanical modeling, the reservoir is assumed to be heterogeneous, isotropic and saturated poro-elastic medium. The reference density of the fluid $\rho_f > 0$ is given and positive.
2. The Lamé coefficients $\lambda > 0$ and $G > 0$, the dimensionless Biot coefficient α, and the pore volume $\varphi*$ are all positive.
3. The fluid is assumed to be slightly compressible and its density is a linear function of pressure. The viscosity $\mu_f > 0$ is assumed to be constant.
4. The absolute permeability tensor, $\boldsymbol{K}$, is assumed to be symmetric, bounded, uniformly positive definite in space and constant in time.
5. The parameters $\boldsymbol{K}$, α, G, M, λ, c_f, μ_f, and φ_0 can vary in space and time.
6. For the fully discrete formulation, we have the following additional assumptions:

   (a) The spatial domain is denoted by $\Omega \subset \mathbb{R}^d$, $d = 1$, 2, or 3. Its external boundary is denoted by $\partial\Omega$, with an outward unit normal vector $\boldsymbol{n}$.
   (b) The spatial domain is discretized into N_Ω conforming grid elements E_i such that: $\overline{\Omega} = \cup_{i=1}^{N_\Omega} E_i$.
   (c) Each grid element E_i has its own, independent, set of flow and mechanics parameters: $\boldsymbol{K}_i$, α_i, G_i, M_i, λ_i, c_{f_i}, μ_{f_i}, and φ_{0_i}. Moreover, we assume that the localized permeabilities $\boldsymbol{K}_i$ include viscosities μ_{f_i} $\left(\text{i.e., } \mathbf{K}_i = \frac{\mathbf{K}_i}{\mu_{f_i}}\right)$.
   (d) The outward normal vector for each grid element E_i is denoted by $\boldsymbol{n}_i$. In addition, for two adjacent grid elements E_i and E_{i-1} sharing a common boundary interface, $\boldsymbol{n}_i = -\boldsymbol{n}_{i-1}$ across the common boundary.

3 | LOCALIZED SINGLE RATE FORMULATION AND ANALYSIS

3.1 | Continuous in space global weak formulation

The continuous in space global weak formulation of the coupled problem reads:

Step (a): Find $p^{n+1,k} \in H^1(\Omega)$, $z^{n+1,k} \in H(\text{div}; \Omega) \cap \{z^{n+1,k} \cdot n = 0 \text{ on } \partial\Omega\}$ such that:

$$\forall \theta \in L^2(\Omega), \sum_{i=1}^{N_\Omega} \left(\left(\left(\frac{1}{M_i} + c_{f_i} \varphi_{0_i} + L_i \right) \left(\frac{p^{n+1,k} - p^{k-1}}{\Delta t} \right) \right), \theta \right)_{E_i} + \sum_{i=1}^{N_\Omega} \left(\nabla \cdot z^{n+1,k}, \theta \right)_{E_i}$$
$$= \sum_{i=1}^{N_\Omega} \left(L_i \left(\frac{p^{n,k} - p^{k-1}}{\Delta t} \right) - \alpha_i \nabla \cdot \left(\frac{u^{n,k} - u^{k-1}}{\Delta t} \right), \theta \right)_{E_i} + \sum_{i=1}^{N_\Omega} (\widetilde{q}, \theta)_{E_i} \tag{10}$$

$$\forall q \in H(\text{div}; \Omega) \cap \{q \cdot n = 0 \text{ on } \partial\Omega\},$$
$$\sum_{i=1}^{N_\Omega} \left(K_i^{-1} z^{n+1,k}, q \right)_{E_i} = \sum_{i=1}^{N_\Omega} \left(p^{n+1,k}, \nabla \cdot q \right)_{E_i}$$
$$- \sum_{i=1}^{N_\Omega} \left\langle p^{n+1,k}, q \cdot n \right\rangle_{\partial E_i} + \sum_{i=1}^{N_\Omega} \left(\nabla \left(\rho_{f,r} g \eta \right), q \right)_{E_i} \tag{11}$$

Step (b): Given $p^{n+1,k}$, $z^{n+1,k}$, find $u^{n+1,k} \in H_0^1(\Omega)^d$ such that,

$$\forall v \in H_0^1(\Omega)^d, \sum_{i=1}^{N_\Omega} 2 \left(G_i \varepsilon \left(u^{n+1,k} \right), \varepsilon(v) \right)_{E_i} + \sum_{i=1}^{N_\Omega} \left(\lambda_i \nabla \cdot u^{n+1,k}, \nabla \cdot v \right)_{E_i}$$
$$- \sum_{i=1}^{N_\Omega} \left(\alpha_i p^{n+1,k}, \nabla \cdot v \right)_{E_i} - \sum_{i=1}^{N_\Omega} \left\langle \sigma \left(u^{n+1,k} \right) n, v \right\rangle_{\partial E_i}$$
$$+ \sum_{i=1}^{N_\Omega} \left\langle \alpha_i p^{n+1,k} \underline{\underline{I}} n, v \right\rangle_{\partial E_i} = \sum_{i=1}^{N_\Omega} (f, v)_{E_i} \tag{12}$$

We note that at the continuum level, the Cauchy stress tensor, given by $\sigma^{por}(u, p) = \sigma(u) - \alpha p \underline{\underline{I}}$, is continuous at grid boundaries. Thus, the boundary terms in Equation (12) can be grouped as:

$$-\sum_{i=1}^{N_\Omega} \left\langle \sigma \left(u^{n+1,k} \right) n, v \right\rangle_{\partial E_i} + \sum_{i=1}^{N_\Omega} \left\langle \alpha_i p^{n+1,k} \underline{\underline{I}} n, v \right\rangle_{\partial E_i} = -\sum_{i=1}^{N_\Omega} \left\langle \sigma^{por} \left(u^{n+1,k} \right) n, v \right\rangle_{\partial E_i} = 0$$

due to the continuity of σ^{por} at grid boundaries and the fact that the normal vector has a different sign in each two adjacent grid elements sharing a common boundary. For the outer boundary, we require that $v = 0$ on $\partial\Omega$.

The boundary term in the flux Equation (11) also vanishes due to similar reasons. The pressure unknown is assumed to be continuous at the continuum level (otherwise ∇p is not defined). In addition, $q \cdot n$ is continuous across element boundaries, as $q \in H(\text{div}; \Omega)$. This results in canceling all inner boundary terms in Equation (11). For outer boundary terms, we restricted the test space such that $q \cdot n = 0$ on $\partial\Omega$. Therefore, we have:

$$\sum_{i=1}^{N_\Omega} \left\langle p^{n+1,k}, q \cdot n \right\rangle_{\partial E_i} = 0.$$

The weak formulation now reads:

Step (a): Find $p^{n+1,k} \in H^1(\Omega)$, $z^{n+1,k} \in H(\text{div}; \Omega) \cap \{z^{n+1,k} \cdot n = 0 \text{ on } \partial\Omega\}$ such that:

$$\forall \theta \in L^2(\Omega), \sum_{i=1}^{N_\Omega} \left(\left(\left(\frac{1}{M_i} + c_{f_i}\varphi_{0_i} + L_i \right) \left(\frac{p^{n+1,k} - p^{k-1}}{\Delta t} \right), \theta \right)_{E_i} + \sum_{i=1}^{N_\Omega} \left(\nabla \cdot z^{n+1,k}, \theta \right)_{E_i}$$

$$= \sum_{i=1}^{N_\Omega} \left(L_i \left(\frac{p^{n,k} - p^{k-1}}{\Delta t} \right) - \alpha_i \nabla \cdot \left(\frac{u^{n,k} - u^{k-1}}{\Delta t} \right), \theta \right)_{E_i} + \sum_{i=1}^{N_\Omega} (\widetilde{q}, \theta)_{E_i} \quad (13)$$

$$\forall q \in H(\text{div}; \Omega) \cap \{q \cdot n = 0 \text{ on } \partial\Omega\},$$

$$\sum_{i=1}^{N_\Omega} \left(K_i^{-1} z^{n+1,k}, q \right)_{E_i} = \sum_{i=1}^{N_\Omega} \left(p^{n+1,k}, \nabla \cdot q \right)_{E_i} + \sum_{i=1}^{N_\Omega} \left(\nabla \left(\rho_{f,r} g \eta \right), q \right)_{E_i} \quad (14)$$

Step (b): Given $p^{n+1,k}, z^{n+1,k}$, find $u^{n+1,k} \in H_0^1(\Omega)^d$ such that,

$$\forall v \in H_0^1(\Omega)^d,$$

$$\sum_{i=1}^{N_\Omega} 2 \left(G_i \varepsilon \left(u^{n+1,k} \right), \varepsilon(v) \right)_{E_i} + \sum_{i=1}^{N_\Omega} \left(\lambda_i \nabla \cdot u^{n+1,k}, \nabla \cdot v \right)_{E_i}$$

$$- \sum_{i=1}^{N_\Omega} \left(\alpha_i p^{n+1,k}, \nabla \cdot v \right)_{E_i} = \sum_{i=1}^{N_\Omega} (f, v)_{E_i} \quad (15)$$

3.2 | Fully discrete weak formulation

Now, we mimic the spatially continuous weak formulation (13)–(15) to obtain the fully discrete formulation (discrete in time and space). We recall that a mixed formulation will be used for flow, and continuous Galerkin will be used for mechanics. Moreover, we assume no flow boundary conditions for the outer flow boundary, and zero displacement boundary conditions for mechanics. The fully-discrete weak formulation now reads:

Step (a): Find $p_h^{n+1,k} \in Q_h$, $z_h^{n+1,k} \in Z_h$ such that:

$$\forall \theta_h \in Q_h, \sum_{i=1}^{N_\Omega} \left(\left(\left(\frac{1}{M_i} + c_{f_i}\varphi_{0_i} + L_i \right) \left(\frac{p_h^{n+1,k} - p_h^{k-1}}{\Delta t} \right), \theta_h \right)_{E_i} + \sum_{i=1}^{N_\Omega} \left(\nabla \cdot z_h^{n+1,k}, \theta_h \right)_{E_i}$$

$$= \sum_{i=1}^{N_\Omega} \left(L_i \left(\frac{p_h^{n,k} - p_h^{k-1}}{\Delta t} \right) - \alpha_i \nabla \cdot \left(\frac{u_h^{n,k} - u_h^{k-1}}{\Delta t} \right), \theta_h \right)_{E_i} + \sum_{i=1}^{N_\Omega} (\widetilde{q}, \theta_h)_{E_i} \quad (16)$$

$$\forall q_h \in Z_h, \sum_{i=1}^{N_\Omega} \left(K_i^{-1} z_h^{n+1,k}, q_h \right)_{E_i} = \sum_{i=1}^{N_\Omega} \left(p_h^{n+1,k}, \nabla \cdot q_h \right)_{E_i} + \sum_{i=1}^{N_\Omega} \left(\nabla \left(\rho_{f,r} g \eta \right), q_h \right)_{E_i} \quad (17)$$

Step (b): Given $p_h^{n+1,k}, z_h^{n+1,k}$, find $u_h^{n+1,k} \in V_h$ such that,

$$\forall v_h \in V_h, \sum_{i=1}^{N_\Omega} 2 \left(G_i \varepsilon \left(u_h^{n+1,k} \right), \varepsilon(v_h) \right)_{E_i} + \sum_{i=1}^{N_\Omega} \left(\lambda_i \nabla \cdot u_h^{n+1,k}, \nabla \cdot v_h \right)_{E_i}$$

$$- \sum_{i=1}^{N_\Omega} \left(\alpha_i p_h^{n+1,k}, \nabla \cdot v_h \right)_{E_i} = \sum_{i=1}^{N_\Omega} (f, v_h)_{E_i} \quad (18)$$

In terms of differences between coupling iterations, equations (16), (17), and (18) read:

$$\forall \theta_h \in Q_h, \frac{1}{\Delta t} \sum_{i=1}^{N_\Omega} \left(\left(\frac{1}{M_i} + c_{f_i} \varphi_{0_i} + L_i \right) \delta p_h^{n+1,k}, \theta_h \right)_{E_i} + \sum_{i=1}^{N_\Omega} \left(\nabla \cdot \delta z_h^{n+1,k}, \theta_h \right)_{E_i}$$

$$= \frac{1}{\Delta t} \sum_{i=1}^{N_\Omega} \left(L_i \delta p_h^{n,k} - \alpha_i \nabla \cdot \delta \boldsymbol{u}_h^{n,k}, \theta_h \right)_{E_i} \tag{19}$$

$$\forall \boldsymbol{q}_h \in \boldsymbol{Z}_h, \sum_{i=1}^{N_\Omega} \left(\boldsymbol{K}_i^{-1} \delta z_h^{n+1,k}, \boldsymbol{q}_h \right)_{E_i} = \sum_{i=1}^{N_\Omega} \left(\delta p_h^{n+1,k}, \nabla \cdot \boldsymbol{q}_h \right)_{E_i} \tag{20}$$

$$\forall \boldsymbol{v}_h \in \boldsymbol{V}_h, \sum_{i=1}^{N_\Omega} 2 \left(G_i \boldsymbol{\varepsilon} \left(\delta \boldsymbol{u}_h^{n+1,k} \right), \boldsymbol{\varepsilon} \left(\boldsymbol{v}_h \right) \right)_{E_i} + \sum_{i=1}^{N_\Omega} \left(\lambda_i \nabla \cdot \delta \boldsymbol{u}_h^{n+1,k}, \nabla \cdot \boldsymbol{v}_h \right)_{E_i}$$

$$- \sum_{i=1}^{N_\Omega} \left(\alpha_i \delta p_h^{n+1,k}, \nabla \cdot \boldsymbol{v}_h \right)_{E_i} = 0 \tag{21}$$

3.3 | Proof of contraction

- **Step 1: Flow equations**

For each grid element E_i, let $\beta_i = \frac{1}{M_i} + c_{f_i} \varphi_{0_i} + L_i$, testing (19) with $\theta_h = \delta p_h^{n+1,k}$, and multiplying by Δt, we obtain:

$$\sum_{i=1}^{N_\Omega} \left\| \beta_i^{1/2} \delta p_h^{n+1,k} \right\|_{E_i}^2 + \Delta t \sum_{i=1}^{N_\Omega} \left(\nabla \cdot \delta z_h^{n+1,k}, \delta p_h^{n+1,k} \right)_{E_i} = \sum_{i=1}^{N_\Omega} \left(L_i \delta p_h^{n,k} - \alpha_i \nabla \cdot \delta \boldsymbol{u}_h^{n,k}, \delta p_h^{n+1,k} \right)_{E_i}. \tag{22}$$

Testing (20) with $\boldsymbol{q}_h = \delta z_h^{n+1,k}$, we obtain:

$$\sum_{i=1}^{N_\Omega} \left(\boldsymbol{K}_i^{-1} \delta z_h^{n+1,k}, \delta z_h^{n+1,k} \right)_{E_i} = \sum_{i=1}^{N_\Omega} \left(\delta p_h^{n+1,k}, \nabla \cdot \delta z_h^{n+1,k} \right)_{E_i}. \tag{23}$$

Substituting (23) into (22), together with Young's inequality, we obtain:

$$\sum_{i=1}^{N_\Omega} \left\| \beta_i^{1/2} \delta p_h^{n+1,k} \right\|_{E_i}^2 + \Delta t \sum_{i=1}^{N_\Omega} \left(\boldsymbol{K}_i^{-1} \delta z_h^{n+1,k}, \delta z_h^{n+1,k} \right)_{E_i}$$

$$\leq \sum_{i=1}^{N_\Omega} \frac{1}{2\epsilon_i} \left\| L_i \delta p_h^{n,k} - \alpha_i \nabla \cdot \delta \boldsymbol{u}_h^{n,k} \right\|_{E_i}^2 + \sum_{i=1}^{N_\Omega} \frac{\epsilon_i}{2} \left\| \delta p_h^{n+1,k} \right\|_{E_i}^2.$$

Introducing a new parameter χ_i for each grid element E_i, we define a local quantity of contraction for each E_i as: $\chi_i \delta \sigma_v^{n,k} = L_i \delta p_h^{n,k} - \alpha_i \nabla \cdot \delta \boldsymbol{u}_h^{n,k}$. The choice $\epsilon_i = \beta_i$ for each E_i gives:

$$\sum_{i=1}^{N_\Omega} \frac{\beta_i}{2} \left\| \delta p_h^{n+1,k} \right\|_{E_i}^2 + \Delta t \sum_{i=1}^{N_\Omega} \left\| \boldsymbol{K}_i^{-1/2} \delta z_h^{n+1,k} \right\|_{E_i}^2 \leq \sum_{i=1}^{N_\Omega} \frac{1}{2\beta_i} \left\| \chi_i \delta \sigma_v^{n,k} \right\|_{E_i}^2. \tag{24}$$

- **Step 2: Elasticity equation**

Now, test the elasticity Equation (21) with $\boldsymbol{v}_h = \delta \boldsymbol{u}_h^{n+1,k}$ to get:

$$\sum_{i=1}^{N_\Omega} 2G_i \left\| \boldsymbol{\varepsilon} \left(\delta \boldsymbol{u}_h^{n+1,k} \right) \right\|_{E_i}^2 + \sum_{i=1}^{N_\Omega} \lambda_i \left\| \nabla \cdot \delta \boldsymbol{u}_h^{n+1,k} \right\|_{E_i}^2 - \sum_{i=1}^{N_\Omega} \alpha_i \left(\delta p_h^{n+1,k}, \nabla \cdot \delta \boldsymbol{u}_h^{n+1,k} \right)_{E_i} = 0. \tag{25}$$

- **Step 3: Combining flow and elasticity equations**

Combining flow (24) with elasticity (25), we obtain:

$$
\sum_{i=1}^{N_\Omega} 2G_i \left\| \boldsymbol{\varepsilon}\left(\delta \boldsymbol{u}_h^{n+1,k}\right) \right\|_{E_i}^2 + \Delta t \sum_{i=1}^{N_\Omega} \left\| \mathbf{K}_i^{-1/2} \delta \boldsymbol{z}_h^{n+1,k} \right\|_{E_i}^2
$$
$$
+ \sum_{i=1}^{N_\Omega} \left\{ \frac{\beta_i}{2} \left\| \delta p_h^{n+1,k} \right\|_{E_i}^2 - \alpha_i \left(\delta p_h^{n+1,k}, \nabla \cdot \delta \boldsymbol{u}_h^{n+1,k}\right)_{E_i} + \lambda_i \left\| \nabla \cdot \delta \boldsymbol{u}_h^{n+1,k} \right\|_{E_i}^2 \right\}
$$
$$
\le \sum_{i=1}^{N_\Omega} \frac{\chi_i^2}{2\beta_i} \left\| \delta \sigma_v^{n,k} \right\|_{E_i}^2. \tag{26}
$$

Now, for each grid element E_i, expand the RHS to match terms on the left hand side and form a square:

$$
\left\| \delta \sigma_v^{n,k} \right\|_{E_i}^2 = \frac{L_i^2}{\chi_i^2} \left\| \delta p_h^{n,k} \right\|_{E_i}^2 - \frac{2\alpha_i L_i}{\chi_i^2} \left(\delta p_h^{n,k}, \nabla \cdot \delta \boldsymbol{u}_h^{n,k}\right)_{E_i} + \frac{\alpha_i^2}{\chi_i^2} \left\| \nabla \cdot \delta \boldsymbol{u}_h^{n,k} \right\|_{E_i}^2.
$$

For each E_i, the following inequalities should be satisfied: $\frac{\beta_i}{2} \ge \frac{L_i^2}{\chi_i^2}$, $\frac{2\alpha_i L_i}{\chi_i^2} = \alpha_i$, and $\lambda_i \ge \frac{\alpha_i^2}{\chi_i^2}$. The first and second inequalities give: $\chi_i^2 = 2L_i$, and $\frac{1}{M_i} + c_{f_i}\varphi_{0_i} \ge 0$, which is trivially satisfied. The third inequality gives: $L_i = \frac{\alpha_i^2}{2\lambda_i}$. With: $L_i = \frac{\alpha_i^2}{2\lambda_i}$ and $\chi_i^2 = 2L_i$, we have:

$$
\sum_{i=1}^{N_\Omega} 2G_i \left\| \boldsymbol{\varepsilon}\left(\delta \boldsymbol{u}_h^{n+1,k}\right) \right\|_{E_i}^2 + \sum_{i=1}^{N_\Omega} \frac{1}{2}\left(\frac{1}{M_i} + c_{f_i}\varphi_{0_i}\right) \left\| \delta p_h^{n+1,k} \right\|_{E_i}^2 + \Delta t \sum_{i=1}^{N_\Omega} \left\| \mathbf{K}_i^{-1/2} \delta \boldsymbol{z}_h^{n+1,k} \right\|_{E_i}^2
$$
$$
+ \sum_{i=1}^{N_\Omega} \left\| \delta \sigma_v^{n+1,k} \right\|_{E_i}^2 \le \sum_{i=1}^{N_\Omega} \left(\frac{L_i}{\frac{1}{M_i} + c_{f_i}\varphi_{0_i} + L_i} \right) \left\| \delta \sigma_v^{n,k} \right\|_{E_i}^2. \tag{27}
$$

We finally have, for each $E_i \in \Omega$, $1 \le i \le N_\Omega$:

$$
2\sum_{i=1}^{N_\Omega} G_i \left\| \boldsymbol{\varepsilon}\left(\delta \boldsymbol{u}_h^{n+1,k}\right) \right\|_{E_i}^2 + \frac{1}{2}\sum_{i=1}^{N_\Omega} \left(\frac{1}{M_i} + c_{f_i}\varphi_{0_i}\right) \left\| \delta p_h^{n+1,k} \right\|_{E_i}^2 + \Delta t \sum_{i=1}^{N_\Omega} \left\| \boldsymbol{K}_i^{-1/2} \delta \boldsymbol{z}_h^{n+1,k} \right\|_{E_i}^2
$$
$$
+ \sum_{i=1}^{N_\Omega} \left\| \delta \sigma_v^{n+1,k} \right\|_{E_i}^2 \le \max_{1 \le i \le N_\Omega} \left(\frac{L_i}{\frac{1}{M_i} + c_{f_i}\varphi_{0_i} + L_i} \right) \sum_{i=1}^{N_\Omega} \left\| \delta \sigma_v^{n,k} \right\|_{E_i}^2. \tag{28}
$$

Theorem 1 *[Localized single rate Banach contraction estimate] The localized multirate iterative scheme is a contraction given by*

$$
2\sum_{i=1}^{N_\Omega} G_i \left\| \boldsymbol{\varepsilon}\left(\delta \boldsymbol{u}_h^{n+1,k}\right) \right\|_{E_i}^2 + \frac{1}{2}\sum_{i=1}^{N_\Omega} \left(\frac{1}{M_i} + c_{f_i}\varphi_{0_i}\right) \left\| \delta p_h^{n+1,k} \right\|_{E_i}^2 + \Delta t \sum_{i=1}^{N_\Omega} \left\| \mathbf{K}_i^{-1/2} \delta \boldsymbol{z}_h^{n+1,k} \right\|_{E_i}^2
$$
$$
+ \sum_{i=1}^{N_\Omega} \left\| \delta \sigma_v^{n+1,k} \right\|_{E_i}^2 \le \max_{1 \le i \le N_\Omega} \left(\frac{L_i}{\frac{1}{M_i} + c_{f_i}\varphi_{0_i} + L_i} \right) \sum_{i=1}^{N_\Omega} \left\| \delta \sigma_v^{n,k} \right\|_{E_i}^2.
$$

4 | LOCALIZED MULTIRATE FORMULATION AND ANALYSIS

In a similar way, we can derive a localized Banach contraction estimate for the multirate case. We start by writing the localized spatially continuous multirate weak formulation. We note that the localized permeability tensor $\boldsymbol{K}_i$ includes the viscosity μ_i.

4.1 | Continuous in space global weak formulation

- Step (a): For $1 \le m \le q$, find $p^{n+1, m+k} \in H^1(\Omega)$, and $z^{n+1, m+k} \in H(\text{div}; \Omega) \cap \{z^{n+1, k} \cdot n = 0 \text{ on } \partial\Omega\}$ such that,

$$
\forall \theta \in L^2(\Omega), \frac{1}{\Delta t} \sum_{i=1}^{N_\Omega} \left(\left(\frac{1}{M_i} + c_{f_i}\varphi_{0_i} + L_i \right) \left(p^{n+1,m+k} - p^{n+1,m-1+k} \right), \theta \right)_{E_i}
$$
$$
+ \sum_{i=1}^{N_\Omega} \left(\nabla \cdot z^{n+1,m+k}, \theta \right)_{E_i} =
$$
$$
\frac{1}{\Delta t} \sum_{i=1}^{N_\Omega} \left(L_i \left(p^{n,m+k} - p^{n,m-1+k} \right) - \frac{\alpha_i}{q} \nabla \cdot \left(\boldsymbol{u}^{n,k+q} - \boldsymbol{u}^{n,k} \right), \theta \right)_{E_i} + \sum_{i=1}^{N_\Omega} (\widetilde{q}, \theta)_{E_i}, \tag{29}
$$

$$
\forall \boldsymbol{q} \in H(\text{div}; \Omega) \cap \{\boldsymbol{q} \cdot n = 0 \text{ on } \partial\Omega\},
$$
$$
\sum_{i=1}^{N_\Omega} \left(\boldsymbol{K}_i^{-1} z^{n+1,m+k}, \boldsymbol{q} \right)_{E_i} = \sum_{i=1}^{N_\Omega} \left(p^{n+1,m+k}, \nabla \cdot \boldsymbol{q} \right)_{E_i}
$$
$$
- \sum_{i=1}^{N_\Omega} \left\langle p^{n+1,m+k}, \boldsymbol{q} \cdot \boldsymbol{n} \right\rangle_{\partial E_i} + \sum_{i=1}^{N_\Omega} \left(\rho_{f,r} g \nabla \eta, \boldsymbol{q} \right)_{E_i}, \tag{30}
$$

- Step (b): Given $p^{n+1,k+q}$ and, $z^{n+1,k+q}$, find $\boldsymbol{u}^{n+1,k+q} \in H_0^1(\Omega)^d$ such that,

$$
\forall \boldsymbol{v} \in H_0^1(\Omega)^d,
$$
$$
2\sum_{i=1}^{N_\Omega} \left(G_i \boldsymbol{\epsilon} \left(\boldsymbol{u}^{n+1,k+q} \right), \boldsymbol{\epsilon}(\boldsymbol{v}) \right)_{E_i} + \sum_{i=1}^{N_\Omega} \left(\lambda_i \nabla \cdot \boldsymbol{u}^{n+1,k+q}, \nabla \cdot \boldsymbol{v} \right)_{E_i} - \sum_{i=1}^{N_\Omega} \left(\alpha_i p^{n+1,k+q}, \nabla \cdot \boldsymbol{v} \right)_{E_i}
$$
$$
- \sum_{i=1}^{N_\Omega} \left\langle \boldsymbol{\sigma} \left(\boldsymbol{u}^{n+1,k+q} \right) \boldsymbol{n}, \boldsymbol{v} \right\rangle_{\partial E_i} + \sum_{i=1}^{N_\Omega} \left\langle \alpha_i p^{n+1,k+q} \underline{\underline{\boldsymbol{I}}} \boldsymbol{n}, \boldsymbol{v} \right\rangle_{\partial E_i} = \sum_{i=1}^{N_\Omega} (\boldsymbol{f}, \boldsymbol{v})_{E_i}. \tag{31}
$$

In a similar way, as detailed in the single rate case, all boundary terms vanish. The continuous-in-space weak formulation then reads:

- Step (a): For $1 \le m \le q$, find $p^{n+1,m+k} \in H^1(\Omega)$, and $z^{n+1,m+k} \in H(\text{div}; \Omega) \cap \{z^{n+1,k} \cdot n = 0 \text{ on } \partial\Omega\}$ such that,

$$
\forall \theta \in L^2(\Omega), \frac{1}{\Delta t} \sum_{i=1}^{N_\Omega} \left(\left(\frac{1}{M_i} + c_{f_i}\varphi_{0_i} + L_i \right) \left(p^{n+1,m+k} - p^{n+1,m-1+k} \right), \theta \right)_{E_i}
$$
$$
+ \sum_{i=1}^{N_\Omega} \left(\nabla \cdot z^{n+1,m+k}, \theta \right)_{E_i} =
$$
$$
\frac{1}{\Delta t} \sum_{i=1}^{N_\Omega} \left(L_i \left(p^{n,m+k} - p^{n,m-1+k} \right) - \frac{\alpha_i}{q} \nabla \cdot \left(\boldsymbol{u}^{n,k+q} - \boldsymbol{u}^{n,k} \right), \theta \right)_{E_i} + \sum_{i=1}^{N_\Omega} (\widetilde{q}, \theta)_{E_i}, \tag{32}
$$

$\forall \boldsymbol{q} \in H(\mathrm{div}; \Omega) \cap \{\boldsymbol{q} \cdot n = 0 \text{ on } \partial\Omega\},$

$$\sum_{i=1}^{N_\Omega} \left(\boldsymbol{K}_i^{-1} \boldsymbol{z}^{n+1,m+k}, \boldsymbol{q}\right)_{E_i} = \sum_{i=1}^{N_\Omega} \left(p^{n+1,m+k}, \nabla \cdot \boldsymbol{q}\right)_{E_i} + \sum_{i=1}^{N_\Omega} \left(\rho_{f,r} g \nabla \eta, \boldsymbol{q}\right)_{E_i}, \tag{33}$$

- Step (b): Given $p^{n+1,k+q}$ and, $\boldsymbol{z}^{n+1,k+q}$, find $\boldsymbol{u}^{n+1,k+q} \in H_0^1(\Omega)^d$ such that,

$\forall \boldsymbol{v} \in H_0^1(\Omega)^d,$

$$2\sum_{i=1}^{N_\Omega} \left(G_i \boldsymbol{\varepsilon} \left(\boldsymbol{u}^{n+1,k+q}\right), \boldsymbol{\varepsilon}(\boldsymbol{v})\right)_{E_i} + \sum_{i=1}^{N_\Omega} \left(\lambda_i \nabla \cdot \boldsymbol{u}^{n+1,k+q}, \nabla \cdot \boldsymbol{v}\right)_{E_i} - \sum_{i=1}^{N_\Omega} \left(\alpha_i p^{n+1,k+q}, \nabla \cdot \boldsymbol{v}\right)_{E_i}$$

$$= \sum_{i=1}^{N_\Omega} (\boldsymbol{f}, \boldsymbol{v})_{E_i}. \tag{34}$$

4.2 | Fully discrete weak formulation

We mimic the spatially continuous weak formulation (32)–(34) and obtain the fully discrete formulation (discrete in time and space) as follows:

- Step (a): For $1 \le m \le q$, find $p_h^{n+1,m+k} \in Q_h$, and $z_h^{n+1,m+k} \in z_h$ such that,

$$\forall \theta_h \in Q_h, \frac{1}{\Delta t} \sum_{i=1}^{N_\Omega} \left(\left(\left(\frac{1}{M_i} + c_{f_i}\varphi_{0_i} + L_i\right)\left(p_h^{n+1,m+k} - p_h^{n+1,m-1+k}\right), \theta_h\right)_{E_i}\right.$$

$$+ \sum_{i=1}^{N_\Omega} \left(\nabla \cdot z_h^{n+1,m+k}, \theta_h\right)_{E_i}$$

$$= \frac{1}{\Delta t} \sum_{i=1}^{N_\Omega} \left(L_i \left(p_h^{n,m+k} - p_h^{n,m-1+k}\right) - \frac{\alpha_i}{q}\nabla \cdot \left(\boldsymbol{u}_h^{n,k+q} - \boldsymbol{u}_h^{n,k}\right), \theta_h\right)_{E_i} + \sum_{i=1}^{N_\Omega} \left(\widetilde{q}_h, \theta_h\right)_{E_i}, \tag{35}$$

$\forall \boldsymbol{q}_h \in \boldsymbol{Z}_h,$

$$\sum_{i=1}^{N_\Omega} \left(\boldsymbol{K}_i^{-1} z_h^{n+1,m+k}, \boldsymbol{q}_h\right)_{E_i} = \sum_{i=1}^{N_\Omega} \left(p_h^{n+1,m+k}, \nabla \cdot \boldsymbol{q}_h\right)_{E_i} + \sum_{i=1}^{N_\Omega} \left(\rho_{f,r} g \nabla \eta, \boldsymbol{q}_h\right)_{E_i}, \tag{36}$$

- Step (b): Given $p_h^{n+1,k+q}$ and, $z_h^{n+1,k+q}$, find $\boldsymbol{u}_h^{n+1,k+q} \in V_h$ such that,

$$\forall \boldsymbol{v}_h \in V_h, 2\sum_{i=1}^{N_\Omega} \left(G_i \boldsymbol{\varepsilon} \left(\boldsymbol{u}_h^{n+1,k+q}\right), \boldsymbol{\varepsilon}\left(\boldsymbol{v}_h\right)\right)_{E_i} + \sum_{i=1}^{N_\Omega} \left(\lambda_i \nabla \cdot \boldsymbol{u}_h^{n+1,k+q}, \nabla \cdot \boldsymbol{v}_h\right)_{E_i}$$

$$- \sum_{i=1}^{N_\Omega} \left(\alpha_i p_h^{n+1,k+q}, \nabla \cdot \boldsymbol{v}_h\right)_{E_i} = \sum_{i=1}^{N_\Omega} \left(\boldsymbol{f}_h, \boldsymbol{v}_h\right)_{E_i}. \tag{37}$$

4.3 | Proof of contraction

- **Step 1: Flow equations**

For each grid element E_i, let $\beta_i = \frac{1}{M_i} + c_{f_i}\varphi_{0_i} + L_i$. For $n \ge 1$, by taking the difference of two successive iterates of (35), which corresponds to one local flow iteration and its corresponding local

flow iteration in the previous flow and geomechanics iterative coupling iteration, testing with $\theta_h = \delta p_h^{n+1,m+k} - \delta p_h^{n+1,m-1+k}$, we obtain

$$
\sum_{i=1}^{N_\Omega} \beta_i \left\| \delta p_h^{n+1,m+k} - \delta p_h^{n+1,m-1+k} \right\|_{E_i}^2
$$
$$
+ \Delta t \sum_{i=1}^{N_\Omega} \left(\nabla \cdot \delta z_h^{n+1,m+k}, \delta p_h^{n+1,m+k} - \delta p_h^{n+1,m-1+k} \right)_{E_i}
$$
$$
= \sum_{i=1}^{N_\Omega} \left(L_i \left(\delta p_h^{n,m+k} - \delta p_h^{n,m-1+k} \right) - \frac{\alpha_i}{q} \nabla \cdot \delta u_h^{n,k+q}, \delta p_h^{n+1,m+k} - \delta p_h^{n+1,m-1+k} \right)_{E_i}. \tag{38}
$$

Similarly, for the flux Equation (36), by taking the difference of two successive iterates, followed by taking the difference at two consecutive finer time steps, $t = t_{m+k}$, and $t = t_{m-1+k}$, and testing with $q_h = \delta z_h^{n+1,m+k}$, we obtain

$$
\sum_{i=1}^{N_\Omega} \left(K_i^{-1} \left(\delta z_h^{n+1,m+k} - \delta z_h^{n+1,m-1+k} \right), \delta z_h^{n+1,m+k} \right)_{E_i}
$$
$$
= \sum_{i=1}^{N_\Omega} \left(\delta p_h^{n+1,m+k} - \delta p_h^{n+1,m-1+k}, \nabla \cdot \delta z_h^{n+1,m+k} \right)_{E_i}. \tag{39}
$$

We combine (38) with (39), apply Young's inequality (for each grid E_i) to obtain

$$
\sum_{i=1}^{N_\Omega} \beta_i \left\| \delta p_h^{n+1,m+k} - \delta p_h^{n+1,m-1+k} \right\|_{E_i}^2
$$
$$
+ \Delta t \sum_{i=1}^{N_\Omega} \left(K_i^{-1} \left(\delta z_h^{n+1,m+k} - \delta z_h^{n+1,m-1+k} \right), \delta z_h^{n+1,m+k} \right)_{E_i}
$$
$$
\leq \sum_{i=1}^{N_\Omega} \frac{1}{2\epsilon_i} \left\| L_i \left(\delta p_h^{n,m+k} - \delta p_h^{n,m-1+k} \right) - \frac{\alpha_i}{q} \nabla \cdot \delta u_h^{n,k+q} \right\|_{E_i}^2
$$
$$
+ \sum_{i=1}^{N_\Omega} \frac{\epsilon_i}{2} \left\| \delta p_h^{n+1,m+k} - \delta p_h^{n+1,m-1+k} \right\|_{E_i}^2.
$$

For each E_i, the choice $\epsilon_i = \beta_i$ absorbs the pressure term on the right hand side. Together with a simple expansion of the flux product, we derive

$$
\sum_{i=1}^{N_\Omega} \frac{\beta_i}{2} \left\| \delta p_h^{n+1,m+k} - \delta p_h^{n+1,m-1+k} \right\|_{E_i}^2
$$
$$
+ \frac{\Delta t}{2} \sum_{i=1}^{N_\Omega} \left\{ \left\| K_i^{-1/2} \delta z_h^{n+1,m+k} \right\|_{E_i}^2 - \left\| K_i^{-1/2} \delta z_h^{n+1,m-1+k} \right\|_{E_i}^2 \right.
$$
$$
+ \left. \left\| K_i^{-1/2} \left(\delta z_h^{n+1,m+k} - \delta z_h^{n+1,m-1+k} \right) \right\|_{E_i}^2 \right\}
$$
$$
\leq \sum_{i=1}^{N_\Omega} \frac{1}{2\beta_i} \left\| L_i \left(\delta p_h^{n,m+k} - \delta p_h^{n,m-1+k} \right) - \frac{\alpha_i}{q} \nabla \cdot \delta u_h^{n,k+q} \right\|_{E_i}^2. \tag{40}
$$

The right hand side constitutes an expression for a quantity to be contracted on. Introducing a new parameter χ_i for each E_i, we define the localized volumetric mean stress for ($1 \le m \le q$) as

$$\chi_i \delta \sigma_v^{n,m+k} = L_i \left(\delta p_h^{n,m+k} - \delta p_h^{n,m-1+k} \right) - \frac{\alpha_i}{q} \nabla \cdot \delta \boldsymbol{u}_h^{n,k+q}. \tag{41}$$

The value of χ_i for each E_i will be chosen such that contraction can be achieved on the spatial summation of the localized norms of $\sigma_v^{n,m+k}$, summed over q flow finer time steps, within one coarser mechanics time step. Summing up (40) for $1 \le m \le q$, substituting the new definition of the localized volumetric mean stress (41), and noting that $\delta z_h^{n+1,k} = 0$, we obtain

$$\sum_{m=1}^{q} \sum_{i=1}^{N_\Omega} \frac{\beta_i}{2} \left\| \delta p_h^{n+1,m+k} - \delta p_h^{n+1,m-1+k} \right\|_{E_i}^2 + \frac{\Delta t}{2} \sum_{i=1}^{N_\Omega} \left\| \boldsymbol{K}_i^{-1/2} \delta z_h^{n+1,k+q} \right\|_{E_i}^2$$

$$+ \frac{\Delta t}{2} \sum_{m=1}^{q} \sum_{i=1}^{N_\Omega} \left\| \boldsymbol{K}_i^{-1/2} \left(\delta z_h^{n+1,m+k} - \delta z_h^{n+1,m-1+k} \right) \right\|_{E_i}^2 \le \sum_{m=1}^{q} \sum_{i=1}^{N_\Omega} \frac{1}{2\beta_i} \left\| \chi_i \delta \sigma_v^{n,m+k} \right\|_{E_i}^2. \tag{42}$$

- **Step 2: Elasticity equation**

For $n \ge 1$, we take the difference of successive iterates of the mechanics Equation (37), and test with $\boldsymbol{v}_h = \delta \boldsymbol{u}_h^{n+1,k+q}$ to get

$$2 \sum_{i=1}^{N_\Omega} G_i \left\| \boldsymbol{\varepsilon} \left(\delta \boldsymbol{u}_h^{n+1,k+q} \right) \right\|_{E_i}^2 + \sum_{i=1}^{N_\Omega} \lambda_i \left\| \nabla \cdot \delta \boldsymbol{u}_h^{n+1,k+q} \right\|_{E_i}^2$$

$$- \sum_{i=1}^{N_\Omega} \alpha_i \left(\delta p_h^{n+1,k+q}, \nabla \cdot \delta \boldsymbol{u}_h^{n+1,k+q} \right)_{E_i} = 0. \tag{43}$$

For the iterative scheme to be contractive, a quantity similar to the right hand side of (42), for the next iterative coupling iteration, $n + 1$, has to be formed. To achieve that, we introduce a term involving a summation over all flow finer time steps in (43) by noticing that

$$\sum_{m=1}^{q} \left(\delta p_h^{n+1,m+k} - \delta p_h^{n+1,m-1+k} \right) = \delta p_h^{n+1,k+q}. \tag{44}$$

Substituting (44) into (43) leads to

$$2 \sum_{i=1}^{N_\Omega} G_i \left\| \boldsymbol{\varepsilon} \left(\delta \boldsymbol{u}_h^{n+1,k+q} \right) \right\|_{E_i}^2 + \sum_{i=1}^{N_\Omega} \lambda_i \left\| \nabla \cdot \delta \boldsymbol{u}_h^{n+1,k+q} \right\|_{E_i}^2$$

$$- \sum_{i=1}^{N_\Omega} \alpha_i \left(\sum_{m=1}^{q} \left(\delta p_h^{n+1,m+k} - \delta p_h^{n+1,m-1+k} \right), \nabla \cdot \delta \boldsymbol{u}_h^{n+1,k+q} \right)_{E_i} = 0. \tag{45}$$

- **Step 3: Combining flow and elasticity equations**

By combining (45) with (42), and rearranging terms, we form a square term, in expanded form, summed over flow finer time steps within one coarser mechanics time step for each grid element E_i,

$$2 \sum_{i=1}^{N_\Omega} G_i \left\| \boldsymbol{\varepsilon} \left(\delta \boldsymbol{u}_h^{n+1,k+q} \right) \right\|_{E_i}^2 + \sum_{m=1}^{q} \sum_{i=1}^{N_\Omega} \left\{ \frac{\beta_i}{2} \left\| \delta p_h^{n+1,m+k} - \delta p_h^{n+1,m-1+k} \right\|_{E_i}^2 \right.$$

$$\left. + \frac{\lambda_i}{q} \left\| \nabla \cdot \delta \boldsymbol{u}_h^{n+1,k+q} \right\|_{E_i}^2 - \alpha_i \left(\delta p_h^{n+1,m+k} - \delta p_h^{n+1,m-1+k}, \nabla \cdot \delta \boldsymbol{u}_h^{n+1,k+q} \right)_{E_i} \right\}$$

$$+ \frac{\Delta t}{2} \sum_{i=1}^{N_\Omega} \left\| K_i^{-1/2} \delta z_h^{n+1,k+q} \right\|_{E_i}^2 + \frac{\Delta t}{2} \sum_{m=1}^{q} \sum_{i=1}^{N_\Omega} \left\| K_i^{-1/2} \left(\delta z_h^{n+1,m+k} - \delta z_h^{n+1,m-1+k} \right) \right\|_{E_i}^2$$

$$\leq \sum_{m=1}^{q} \sum_{i=1}^{N_\Omega} \frac{\chi_i^2}{2\beta_i} \left\| \delta \sigma_v^{n,m+k} \right\|_{E_i}^2. \tag{46}$$

It remains to choose the values of our newly introduced parameters, χ_i and L_i, such that the coefficients of the expanded square contributes only positive terms to the left hand side of (46). Therefore, we expand the right hand side of (46) for each E_i as

$$\left\| \delta \sigma_v^{n,m+k} \right\|_{E_i}^2 = \frac{L_i^2}{\chi_i^2} \left\| \delta p_h^{n,m+k} - \delta p_h^{n,m-1+k} \right\|_{E_i}^2$$

$$- \frac{2\alpha_i L_i}{q\chi_i^2} \left(\delta p_h^{n,m+k} - \delta p_h^{n,m-1+k}, \nabla \cdot \delta u_h^{n,k+q} \right)_{E_i} + \frac{\alpha_i^2}{\chi_i^2 q^2} \left\| \nabla \cdot \delta u_h^{n,k+q} \right\|_{E_i}^2. \tag{47}$$

Now, we match the coefficients of the expansion in (47) to the coefficients of the expanded square on the right hand side of (46), hence, deduce the values of χ_i and L_i for each grid element E_i, respectively. For the left hand side of (46) to remain positive, the following inequalities should be satisfied

$$\frac{\beta_i}{2} \geq \frac{L_i^2}{\chi_i^2}, \frac{2\alpha_i L_i}{q\chi_i^2} = \alpha_i, \frac{\lambda_i}{q} \geq \frac{\alpha_i^2}{\chi_i^2 q^2}.$$

The second and third inequalities give rise to the following condition

$$L_i \geq \frac{\alpha_i^2}{2\lambda_i} \text{ for each } E_i.$$

The first inequality gives rise to $q \leq \frac{\beta_i}{L_i}$. For $L_i = \frac{\alpha_i^2}{2\lambda_i}, \chi_i^2 = \frac{\alpha_i^2}{q\lambda_i}$, we derive the following condition on the number of flow finer time steps within one coarse mechanics time step

$$q \leq \frac{2\lambda_i}{\alpha_i^2} \left(\frac{1}{M_i} + c_{f_i} \varphi_{0_i} \right) + 1 \text{ for each } E_i, \tag{48}$$

which is not restrictive as typically in practice the values of λ_i are quite large. Now, we group the terms of the expanded square on the left hand side of (46) to form the quantity of contraction for the next iterative coupling iteration, $n+1$, as

$$2 \sum_{i=1}^{N_\Omega} G_i \left\| \varepsilon \left(\delta u_h^{n+1,k+q} \right) \right\|_{E_i}^2 + \sum_{m=1}^{q} \sum_{i=1}^{N_\Omega} \left(\frac{\beta_i}{2} - \frac{L_i^2}{\chi_i^2} \right) \left\| \delta p_h^{n+1,m+k} - \delta p_h^{n+1,m-1+k} \right\|_{E_i}^2$$

$$+ \sum_{m=1}^{q} \sum_{i=1}^{N_\Omega} \left\| \delta \sigma_v^{n+1,m+k} \right\|_{E_i}^2 + \frac{\Delta t}{2} \sum_{i=1}^{N_\Omega} \left\| K_i^{-1/2} \delta z_h^{n+1,k+q} \right\|_{E_i}^2$$

$$+ \frac{\Delta t}{2} \sum_{m=1}^{q} \sum_{i=1}^{N_\Omega} \left\| K_i^{-1/2} \left(\delta z_h^{n+1,m+k} - \delta z_h^{n+1,m-1+k} \right) \right\|_{E_i}^2 \leq \sum_{m=1}^{q} \sum_{i=1}^{N_\Omega} \frac{\chi_i^2}{2\beta_i} \left\| \delta \sigma_v^{n,m+k} \right\|_{E_i}^2.$$

Substituting $\chi_i^2 = \frac{2L_i}{q}, \beta_i = \frac{1}{M_i} + c_{f_i} \varphi_{0_i} + L_i$ for each E_i, with further algebraic simplifications, we obtain

$$2 \sum_{i=1}^{N_\Omega} G_i \left\| \varepsilon \left(\delta u_h^{n+1,k+q} \right) \right\|_{E_i}^2$$

$$+ \frac{1}{2} \sum_{m=1}^{q} \sum_{i=1}^{N_\Omega} \left(\frac{1}{M_i} + c_{f_i} \varphi_{0_i} + (1-q)L_i \right) \left\| \delta p_h^{n+1,m+k} - \delta p_h^{n+1,m-1+k} \right\|_{E_i}^2$$

$$+ \frac{\Delta t}{2} \sum_{i=1}^{N_\Omega} \left\| K_i^{-1/2} \delta z_h^{n+1,k+q} \right\|_{E_i}^2 + \frac{\Delta t}{2} \sum_{m=1}^{q} \sum_{i=1}^{N_\Omega} \left\| K_i^{-1/2} \left(\delta z_h^{n+1,m+k} - \delta z_h^{n+1,m-1+k} \right) \right\|_{E_i}^2$$

$$+ \sum_{m=1}^{q} \sum_{i=1}^{N_\Omega} \left\| \delta \sigma_v^{n+1,m+k} \right\|_{E_i}^2 \leq \max_{1 \leq i \leq N_\Omega} \left(\frac{L_i}{q \left(\frac{1}{M_i} + c_{f_i} \varphi_{0_i} + L_i \right)} \right) \sum_{m=1}^{q} \sum_{i=1}^{N_\Omega} \left\| \delta \sigma_v^{n,m+k} \right\|_{E_i}^2. \tag{49}$$

The contraction coefficient: $\max_{1 \leq i \leq N_\Omega} \left(\frac{L_i}{q \left(\frac{1}{M_i} + c_{f_i} \varphi_{0_i} + L_i \right)} \right) < 1$ for $q \geq 1$. This is trivially satisfied (at least we take one flow time step followed by one mechanics time step).

Theorem 2 *[Localized multirate contraction estimate] For* $q \leq 1 + \min_{1 \leq i \leq N_\Omega} \frac{2\lambda_i}{\alpha_i^2} \left(\frac{1}{M_i} + c_{f_i} \varphi_{0_i} \right), L_i = \frac{\alpha_i^2}{2\lambda_i}$ *and* $\chi_i^2 = \frac{2L_i}{q}$, *the localized multirate iterative scheme is a contraction given by*

$$2 \sum_{i=1}^{N_\Omega} G_i \left\| \varepsilon \left(\delta u_h^{n+1,k+q} \right) \right\|_{E_i}^2$$

$$+ \frac{1}{2} \sum_{m=1}^{q} \sum_{i=1}^{N_\Omega} \left(\frac{1}{M_i} + c_{f_i} \varphi_{0_i} + (1-q)L_i \right) \left\| \delta p_h^{n+1,m+k} - \delta p_h^{n+1,m-1+k} \right\|_{E_i}^2$$

$$+ \frac{\Delta t}{2} \sum_{i=1}^{N_\Omega} \left\| K_i^{-1/2} \delta z_h^{n+1,k+q} \right\|_{E_i}^2$$

$$+ \frac{\Delta t}{2} \sum_{m=1}^{q} \sum_{i=1}^{N_\Omega} \left\| K_i^{-1/2} \left(\delta z_h^{n+1,m+k} - \delta z_h^{n+1,m-1+k} \right) \right\|_{E_i}^2 + \sum_{m=1}^{q} \sum_{i=1}^{N_\Omega} \left\| \delta \sigma_v^{n+1,m+k} \right\|_{E_i}^2$$

$$\leq \max_{1 \leq i \leq N_\Omega} \left(\frac{L_i}{q \left(\frac{1}{M_i} + c_{f_i} \varphi_{0_i} + L_i \right)} \right) \sum_{m=1}^{q} \sum_{i=1}^{N_\Omega} \left\| \delta \sigma_v^{n,m+k} \right\|_{E_i}^2.$$

5 | MULTIRATE BANACH CONTRACTION ESTIMATES FOR HOMOGENEOUS VERSUS HETEROGENEOUS (LOCALIZED) POROELASTIC MEDIA

Table 1 compares the Banach contraction result derived for the multirate scheme in homogeneous poroelastic media [3] against the one derived in this article (for heterogeneous poro-elastic media).

Remark 2 Our localized Banach estimates work provides another strong justification for introducing the modified multirate iterative coupling scheme presented in our earlier work [3]. Following a similar approach to the proof presented above, the localized modified multirate iterative coupling scheme will not impose any upper bound on the number of flow finer time steps taken within one coarse mechanics time steps. This follows immediately as the quantity of contraction in the modified scheme is independent of q. The details are spared.

Remark 3 For our earlier obtained results, the word "homogeneous" is not as restrictive as it sounds. In fact, some degree of uniformity in the flow and mechanics parameters should be imposed in this case. However, parameter values can change smoothly across

TABLE 1 Banach contraction estimates for homogeneous versus heterogeneous (localized) poro-elastic media.

	Original contraction estimates for poroelastic media	Localized contraction estimates for heterogeneous poroelastic media
Conditions on parameters	A degree of spatial uniformity should be imposed as described in Remark 3	Parameters can be heterogeneous
Contraction coefficient	$\left(\frac{L}{\frac{1}{M}+c_f\varphi_0+L}\right)^2$	$\max_{1\leq i\leq N_\Omega}\left(\frac{L_i}{q\left(\frac{1}{M_i}+c_{f_i}\varphi_{0_i}+L_i\right)}\right)$ for $L_i=\frac{\alpha_i^2}{2\lambda_i}$ for all $E_i\in\Omega$
Condition on q	None	$q\leq 1+\min_{1\leq i\leq N_\Omega}\frac{2\lambda_i}{\alpha_i^2}\left(\frac{1}{M_i}+c_{f_i}\varphi_{0_i}\right)$
When do contraction coefficients Match?	For $L=\frac{\alpha^2}{2\lambda}$, $\left(\frac{M\alpha^2}{2(\lambda+M\lambda c_f\varphi_0)+M\alpha^2}\right)^2$	For $q=$ upper limit, and $L_i=\frac{\alpha_i^2}{2\lambda_i}$ for all $E_i\in\Omega$, contraction estimate $=\max_{1\leq i\leq N_\Omega}\left(\frac{M_i\alpha_i^2}{2\left(\lambda_i+M_i\lambda_i c_{f_i}\varphi_{0_i}\right)+M_i\alpha_i^2}\right)^2$. Exact match

the spatial domain. The fixed stress stabilization term in this case should take the form $L=\frac{\alpha_{max}^2}{2\lambda_{min}}$, and this value will be added to the main diagonal of the linear system in a homogeneous manner. In fact, this leads to slower convergence rate, as the contraction coefficient increases monotonically with L. The power of the localized contraction result is that it allows us to add localized fixed-stress regularization terms which can vary across grid cells, yet the scheme is still contractive.

6 | NUMERICAL RESULTS

6.1 | Brugge field model

We consider the Brugge field model [2, 51] with a heterogeneous permeability distribution for comparing the efficiency of the multirate scheme versus the single rate scheme. The model consists of a $9\times 48\times 139$ general hexahedral elements capturing the field geometry, with 30 bottom-hole pressure specified wells, 10 of which are injectors at a pressure of 2600 psi, and 20 are producers at a pressure of 1000 psi. Producers are located at a lower elevation compared to injectors. No flow boundary condition is enforced across all external boundaries. For the mechanics model, we apply a mixture of zero displacement and traction boundary conditions. Gravity is not neglected in the model and detailed specifications of the input parameters can be found in Table 2.

6.2 | Results

Figures 2 and 3 show the pressure profiles after 16 and 192 days of simulation for the single rate and multirate schemes ($q=1$, 2, 4, and 8). All four schemes result in almost identical results. We also note that the upper bound for q is calculated to be: $q\leq 1+\min_{1\leq i\leq N_\Omega}\frac{2\lambda_i}{\alpha_i^2}\left(\frac{1}{M_i}+c_{f_i}\varphi_{0_i}\right)=10.52$. That is, for the multirate scheme to be theoretically convergent, we should choose $q\leq 10$. In other words, we should not take more than 10 finer time steps within one coarse mechanics time steps for the iteration to converge. This upper bound is validated numerically as follows: we will show in the second paragraph that for $q\leq 8$, the number of iterative coupling iterations increase, which in turn increase the number of flow and mechanics linear iterations, and the overall CPU runtime as well. Therefore, for the multirate fixed stress split scheme to converge faster and be effective, we should not exceed 8 flow fine time steps within one course mechanics time step. This is predicted by our computed upper bound $q\leq 10$.

Figure 4a shows the accumulated CPU run time for the single rate case ($q=1$), and for multirate cases: $q=2$, 4, and 8. The multirate iterative coupling algorithm with two flow finer time steps within

TABLE 2 Input parameters for Brugge field model.

Injectors wells	10 injectors (pressure specified at 2600.0 psi)
Producers wells	20 producers (pressure specified at 1000.0 psi)
Total simulation time	192.0 days
Finer (unit) time step	1.0 days
Number of grids	60048 grids ($9 \times 48 \times 139$)
Permeabilities	highly varying
k_{xx}	Range: (0.002122, 350.1372) md
k_{yy}	Range: (0.022143, 4135.124) md
k_{zz}	Range: (0.022493, 4163.053) md
Initial porosity, φ_0	0.2
Fluid viscosity, μ_f	2.0 cp
Initial pressure, p_0	400.0 psi
Fluid compressibility c_f:	1.E-4 (1/psi)
Rock compressibility:	1.E-6 (1/psi)
Rock density:	165.44 lb_m/ft^3
Initial fluid density, ρ_f:	56.0 lb_m/ft^3
Young's modulus (E)	1.E5 psi
Poisson ratio, ν	0.4
Biot's constant, α	0.6
Biot modulus, M	1.0E16 psi
$\lambda = \frac{E\nu}{(1+\nu)(1-2\nu)}$	142857.0 psi
L (introduced fixed stress parameter)	$\frac{\alpha^2}{2\lambda}$
Flow boundary conditions	No flow boundary condition on all 6 boundaries
Mechanics B.C.	
"X+" boundary (EBCXX1())	$\sigma_{xx} = \sigma \cdot n_x = 5,000\ psi$, (overburden pressure)
"X-" - boundary (EBCXXN1())	$\boldsymbol{u} = 0$, zero displacement
"Y+" - boundary (EBCYY1())	$\sigma_{yy} = \sigma \cdot n_y = 1500\ psi$
"Y-" - boundary (EBCYYN1())	$\boldsymbol{u} = 0$, zero displacement
"Z+" - boundary (EBCZZ1())	$\boldsymbol{u} = 0$, zero displacement
"Z-" - boundary (EBCZZN1())	$\sigma_{zz} = \sigma \cdot n_z = 1000\ psi$

one coarser mechanics time step ($q = 2$) results in 27.32% reduction in CPU run time compared to the single rate. Multirate couplings ($q = 4$, and $q = 8$) result in 48.43%, and 51.15% reductions in CPU run times respectively. Figure 4b explains the reduction in CPU run time observed in the multirate case. By just solving for two flow finer time steps within one coarser mechanics time step ($q = 2$), the total number of mechanics linear iterations was reduced by 51.08% with reference to the single rate case. Multirate couplings ($q = 4$, and $q = 8$) result in 75.61%, and 86.29% reductions in the number of mechanics linear iterations respectively, which in turn, reduce the CPU run time as well. Figure 4c shows the total number of flow linear iterations in the four cases. We see an increase in the total number of flow linear iterations for multirate iterative couplings. Multirate iterative coupling with two flow finer time steps ($q = 2$), within one coarse mechanics time step results in 44.76% increase in the total number of flow linear iterations. Multirate couplings ($q = 2$), and ($q = 8$) result in 49.63%, and 69.01% increase in the total number of flow linear iterations respectively. Figure 4d shows the number of iterative coupling iterations per coarse mechanics time step. The increase in the number of flow linear iterations for multirate cases is attributed to the increase in the number of iterative coupling iterations performed for each coarse mechanics time step, as shown in Figure 4d. This validates the
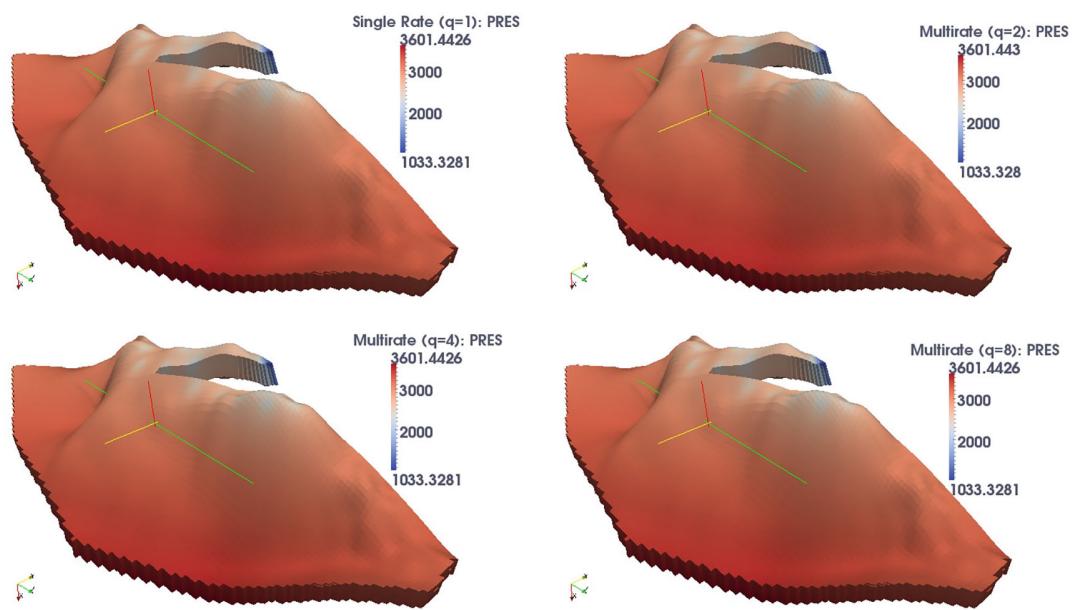
FIGURE 2   Pressure profiles after 16.0 simulation days.
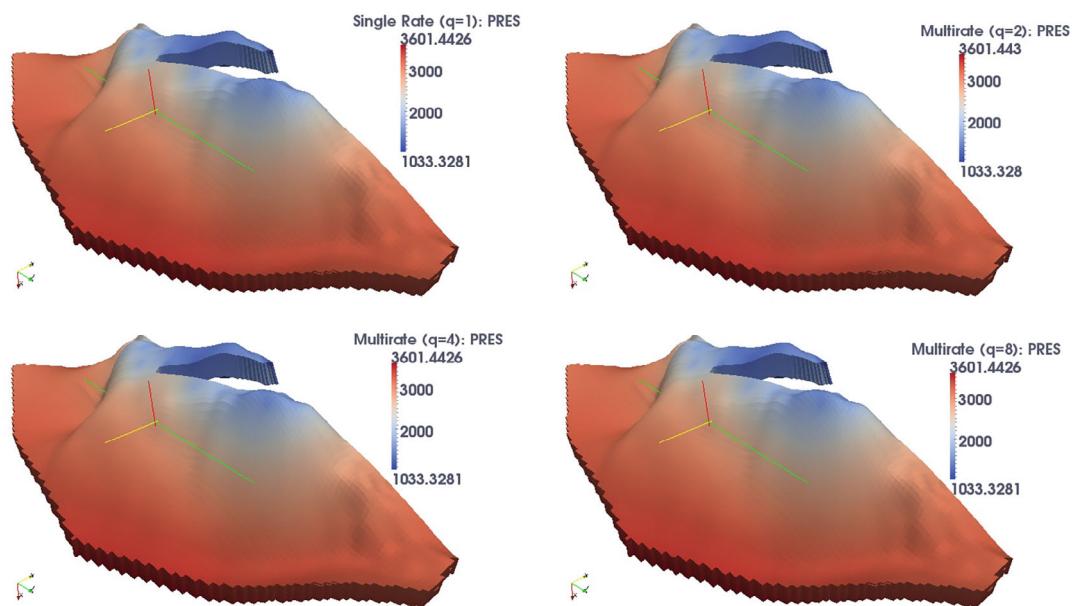
FIGURE 3   Pressure profiles after 192.0 simulation days.

theoretical upper bound on $q(q \leq 10)$, or the number of flow fine time steps taken within one coarse mechanics time step, as discussed in the previous paragraph. In addition, the huge decrease in the number of mechanics linear iterations outperform the overhead introduced by the increase in the number of flow linear iterations. This is a key factor to the success of the iterative multirate coupling scheme in reducing the overall CPU run time.
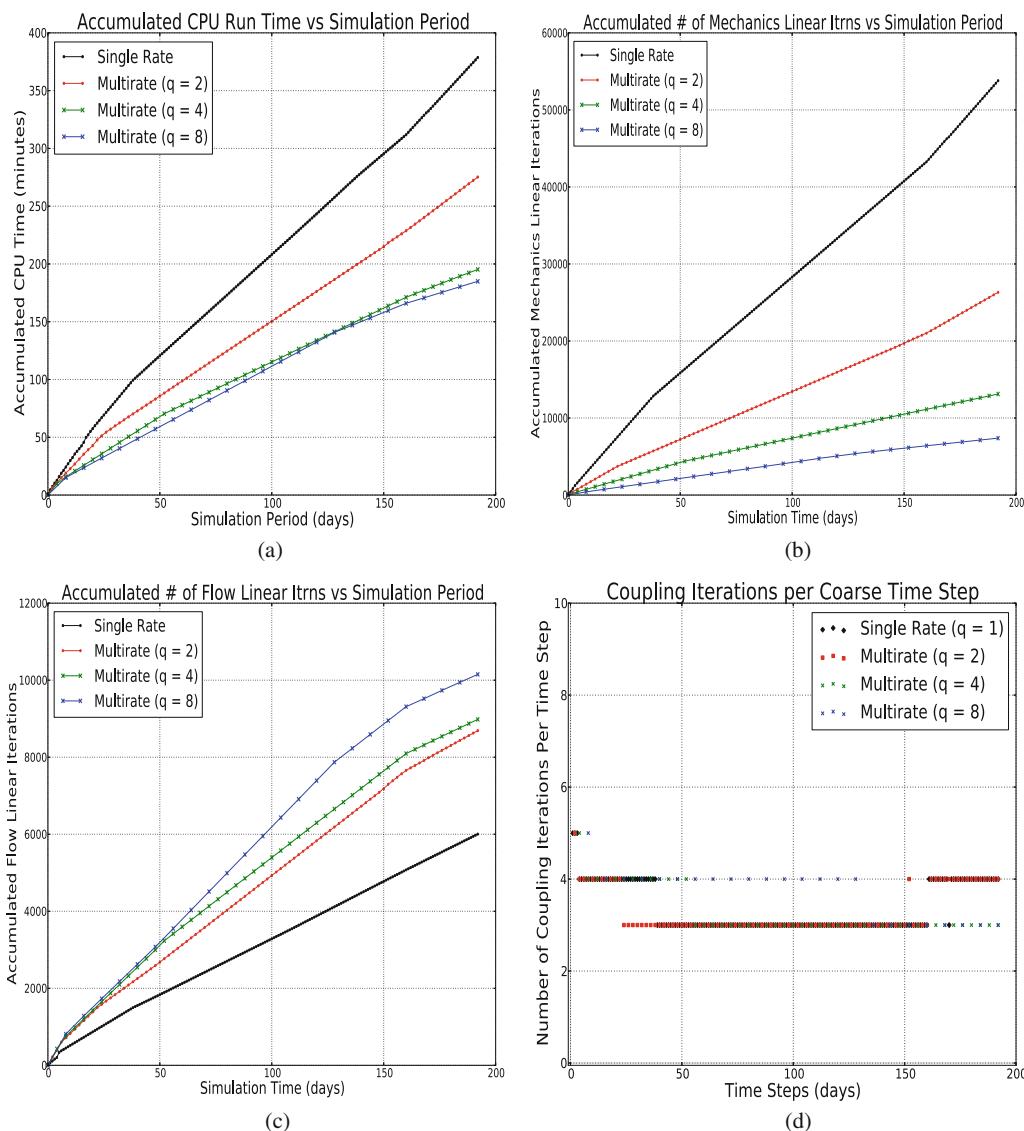
FIGURE 4 Brugge field model results. (a) CPU run time versus simulation days; (b) total number of mechanics linear iterations versus simulation days; (c) total number of flow linear iterations versus simulation days; (d) number of iterative coupling iterations per coarser time step.

We conclude that the applicability and efficiency of the multirate fixed-stress split iterative coupling scheme extends to the case in which the poro-elastic media is highly heterogeneous. Its convergence is shown theoretically, and observed numerically for field-scale problems, with a heterogeneous permeability distribution.

7 | CONCLUSIONS AND OUTLOOK

This article considers single rate and multirate fixed stress split iterative coupling schemes in heterogeneous poroelastic media. The fixed stress split scheme allows for the sequential coupling

of flow with mechanics and a coupling iteration is imposed until convergence is obtained for every discrete time step. The convergence of both the single rate and multirate coupling schemes in homogeneous poroelastic media have been established in the past [3]. The novelty of the work presented in this article is that it extends these Banach contraction results to the case in which the poroelastic media is highly heterogeneous (flow and mechanics parameters can vary in both space and time). To the best of our knowledge, this is the first time in literature a Banach contraction result has been rigorously obtained for the multirate fixed stress split iterative coupling scheme in heterogeneous poroelastic media. Moreover, the localized contraction proof outlines a general strategy that is very likely to be applicable for obtaining similar localized contraction estimates for other iterative coupling schemes, as shown in [8] for example for the undrained split scheme. In addition, our analysis reveals an upper bound on the number of flow fine time steps that can be solved for within one coarse mechanics time step in the multirate scheme. Our theoretical findings in this article are supplemented by numerical results for a realistic reservoir model with a highly heterogenous permeability field, validating the derived upper bound in the multirate case. In addition, the numerical results show that the applicability and efficiency of the multirate scheme extends to the case in which the poroelastic medium is highly heterogeneous.

DATA AVAILABILITY STATEMENT
Research data are not shared in this study.

ORCID
Tameem Almani 🔳 https://orcid.org/0000-0002-5603-2533

REFERENCES

[1] E. Ahmed, J. M. Nordbotten, and F. A. Radu, *Adaptive asynchronous time-stepping, stopping criteria, and a posteriori error estimates for fixed-stress iterative schemes for coupled poromechanics problems*, J. Comput. Appl. Math. 364 (2020), 112312.

[2] T. Almani, Efficient algorithms for flow models coupled with Geomechanics for porous media applications, Ph.D. thesis, The University of Texas at Austin, 2016.

[3] T. Almani, K. Kumar, A. Dogru, G. Singh, and M. F. Wheeler, *Convergence analysis of multirate fixed-stress split iterative schemes for coupling flow with geomechanics*, Comput. Methods Appl. Mech. Eng. 311 (2016), 180–207.

[4] T. Almani, K. Kumar, G. Singh, and M. F. Wheeler, *Stability of multirate explicit coupling of geomechanics with flow in a poroelastic medium*, Comput. Math. Appl. 78 (2019), no. 8, 2682–2699.

[5] T. Almani, K. Kumar, G. Singh, and M. F. Wheeler. *Convergence and error analysis of fully discrete iterative coupling schemes for coupling flow with geomechanics*, 15th Eur. Conf. Math. Oil Recover. (ECMOR XV), Aug. 29–Sept. 1, 2016.

[6] T. Almani, K. Kumar, and M. F. Wheeler, *Convergence and error analysis of fully discrete iterative coupling schemes for coupling flow with geomechanics*, Comput. Geosci. 21 (2017), 1157–1172.

[7] T. Almani, S. Lee, M. F. Wheeler, and T. Wick, *Multirate coupling for flow and geomechanics applied to hydraulic fracturing using an adaptive phase-field technique*, SPE Reserv. Simul. Conf., Houston, TX, February 20-22, 2017.

[8] T. Almani, A. Manea, K. Kumar, and A. H. Dogru, *Convergence of the undrained split iterative scheme for coupling flow with geomechanics in heterogeneous poroelastic media*, Comput. Geosci. 24 (2020), 551–569.

[9] M. A. Biot, *Consolidation settlement under a rectangular load distribution*, J. Appl. Phys. 12 (1941), no. 5, 426–430.

[10] M. A. Biot, *General theory of three-dimensional consolidation*, J. Appl. Phys. 12 (1941), no. 2, 155–164.

[11] P. B. Bochev and D. Ridzal, *An optimization-based approach for the design of PDE solution algorithms*, SIAM J. Numer. Anal. 47 (2009), no. 5, 3938–3955.

[12] M. Borregales, K. Kumar, F. A. Radu, C. Rodrigo, and F. J. Gaspar, *A partially parallel-in-time fixed-stress splitting method for Biot's consolidation model*, Comput. Math. Appl. 77 (2019), no. 6, 1466–1478.

[13] M. Borregales, F. A. Radu, K. Kumar, and J. M. Nordbotten, *Robust iterative schemes for non-linear poromechanics*, Comput. Geosci. 22 (2018), no. 4, 1021–1038.

[14] J. W. Both, M. Borregales, J. M. Nordbotten, K. Kumar, and F. A. Radu, *Robust fixed stress splitting for biots equations in heterogeneous media*, Appl. Math. Lett. 68 (2017), 101–108.

[15] J. W. Both, K. Kumar, J. M. Nordbotten, and F. A. Radu, *Anderson accelerated fixed-stress splitting schemes for consolidation of unsaturated porous media*, Comput. Math. Appl. 77 (2019), no. 6, 1479–1502.

[16] J. W. Both, K. Kumar, J. M. Nordbotten, and F. A. Radu, *The gradient flow structures of thermo-poro-visco-elastic processes in porous media*, arXiv:1907.03134, 2019.

[17] L. D. Carciopolo, L. Formaggia, A. Scotti, and H. Hajibeygi, *Conservative multirate multiscale simulation of multiphase flow in heterogeneous porous media*, J. Comput. Phys. 404 (2020), 109134.

[18] N. Castelletto, J. A. White, and H. A. Tchelepi, *Accuracy and convergence properties of the fixed-stress iterative solution of two-way coupled poromechanics*, Int. J. Numer. Anal. Methods Geomech. 39 (2015), no. 14, 1593–1618.

[19] L. Y. Chin, R. Raghaven, and L. K. Thomas, *Fully-coupled geomechanics and fluid-flow analysis of wells with stress-dependent permeability*, 1998 SPE Int. Conf. Exhib., Beijing, China, November 2-6, 1998.

[20] L. Y. Chin, L. K. Thomas, J. E. Sylte, and R. G. Pierson, *Iterative coupled analysis of geomechanics and fluid flow for rock compaction in reservoir simulation*, Oil Gas Sci. Technol. 57 (2002), no. 5, 485–497.

[21] O. Coussy, *A general theory of thermoporoelastoplasticity for saturated porous materials*, Transp. Porous Media 4 (1989), 281–293.

[22] S. Dana, B. Ganis, and M. F. Wheeler, *A multiscale fixed stress split iterative scheme for coupled flow and poromechanics in deep subsurface reservoirs*, J. Comput. Phys. 352 (2018), 1–22.

[23] S. Dana and M. F. Wheeler. *Convergence analysis of fixed stress split iterative scheme for small strain anisotropic poroelastoplasticity: A primer*, arXiv:1810.04163, 2018.

[24] L. S. K. Fung, L. Buchanan, and R. G. Wan, *Coupled geomechanical-thermal simulation for deforming heavy-oil reservoirs*, J. Can. Pet. Technol. 33 (1994), no. 4, PETSOC-94-04-03.

[25] X. Gai, *A coupled geomechanics and reservoir flow model on parallel computers*, Ph.D. thesis, The University of Texas at Austin, 2004.

[26] X. Gai, R. H. Dean, M. F. Wheeler, and R. Liu. *Coupled geomechanical and reservoir modeling on parallel computers*. The SPE Reserv. Simul. Symp., Houston, TX, February 3–5, 2003.

[27] F. J. Gaspar and C. Rodrigo, *On the fixed-stress split scheme as smoother in multigrid methods for coupling flow and geomechanics*, Comput. Methods Appl. Mech. Eng. 326 (2017), 526–540.

[28] J. Geertsma, *Problems of rock mechanics in petroleum production engineering*, Proc. First Congr. Int. Soc. Rock Mech., Lisbon, 1996, pp. 585–594.

[29] V. Girault, M. F. Wheeler, T. Almani, and S. Dana. *A priori error estimates for a discretized poro-elastic–elastic system solved by a fixed-stress algorithm*, Oil Gas Sci. Technol. 74 (2019), 24.

[30] V. Girault, M. F. Wheeler, B. Ganis, and M. E. Mear, *A lubrication fracture model in a poro-elastic medium*, Math. Models Methods Appl. Sci. 25 (2015), no. 4, 587–645.

[31] Q. Hong, J. Kraus, M. Lymbery, and M. F. Wheeler, *Parameter-robust convergence analysis of fixed-stress split iterative method for multiple-permeability poroelasticity systems*, Multiscale Model. Simul. 18 (2020), no. 2, 916–941.

[32] J. Hoy, I. Tezaur, and A. Mota. "The schwarz alternating method for multiscale contact mechanics," *CSRI summer proceedings 2021*, E. Galvan and D. Smith (eds.), Technical report SAND2021-9886C, Sandia National Laboratories, 2021.

[33] J. Kim, H. A. Tchelepi, and R. Juanes, *Stability, accuracy, and efficiency of sequential methods for coupled flow and geomechanics*, SPE J. 16 (2009), 249–262.

[34] J. Kim, H. A. Tchelepi, and R. Juanes, *Stability and convergence of sequential methods for coupled flow and geomechanics: Drained and undrained splits*, Comput. Methods Appl. Mech. Eng. 200 (2011), no. 23–24, 2094–2116.

[35] J. Kim, H. A. Tchelepi, and R. Juanes, *Stability and convergence of sequential methods for coupled flow and geomechanics: Fixed-stress and fixed-strain splits*, Comput. Methods Appl. Mech. Eng. 200 (2011), no. 13–16, 1591–1606.

[36] K. Kumar, T. Almani, G. Singh, and M. F. Wheeler, "Multirate undrained splitting for coupled flow and geomechanics in porous media," *Numerical mathematics and advanced applications ENUMATH 2015*, B. Karasözen,

M. Manguoğlu, M. Tezer-Sezgin, S. Göktepe, and Ö. Uğur (eds.), Springer International Publishing, Cham, 2016, pp. 431–440.

[37] K. Kumar, S. Kyas, J. M. Nordbotten, and S. Repin, *Guaranteed and computable error bounds for approximations constructed by an iterative decoupling of the Biot problem*, Comput. Math. Appl. 91 (2020), 122–149.

[38] J. L. Lions, *Virtual and effective control for distributed systems and decomposition of everything*, J. d'Analyse Math. 80 (2000), 257–297.

[39] J. L. Lions and O. Pironneau, *Virtual control, replicas and decomposition of operators*, Comptes Rendus l'Academie Des Sci. I Math. 330 (2000), no. 1, 47–54.

[40] A. Mikelić, B. Wang, and M. F. Wheeler, *Numerical convergence study of iterative coupling for coupled flow and geomechanics*, Comput. Geosci. 18 (2014), 325–341.

[41] A. Mikelić and M. F. Wheeler, *Convergence of iterative coupling for coupled flow and geomechanics*, Comput. Geosci. 17 (2013), 455–461.

[42] A. Mota, I. Tezaur, and A. Coleman, *The schwarz alternating method in solid mechanics*, Comput. Methods Appl. Mech. Eng. 319 (2017), 19–51.

[43] A. Mota, I. Tezaur, and G. Phlipot, *The Schwarz alternating method for transient solid dynamics*, Int. J. Numer. Meth. Eng. 123(2022), 5036–5071.

[44] M. A. Murad, M. R. Correa, M. R. Borges, J. A. Luízar-Obregón, and T. V. Lopes, *A fixed-stress split strategy for two-phase flow in heterogeneous poroelastic media overlain by viscoelastic rock salt layers*, Comput. Methods Appl. Mech. Eng. 380 (2021), 113768.

[45] R. Quevedo and D. Roehl, *A novel iterative method based on fixed stress rates for hydromechanical problems with nonlinear constitutive relationships*, Comput. Geotech. 130 (2021), 103887.

[46] J. R. Rice and M. P. Cleary, *Some basic stress diffusion solutions for fluid-saturated elastic porous media with compressible constituents*, Rev. Geophys. Space Phys. 14 (1976), 227.

[47] I. Rybak, J. Magiera, R. Helmig, and C. Rohde, *Multirate time integration for coupled saturated/unsaturated porous medium and free flow systems*, Comput. Geosci. 19 (2015), no. 2, 299–309.

[48] V. Savcenco, W. Hundsdorfer, and J. G. Verwer, *A multirate time stepping strategy for stiff ordinary differential equations*, BIT Numer. Math. 47 (2007), no. 1, 137–155.

[49] A. Settari and F. M. Mourits, *Coupling of geomechanics and reservoir simulation models*, Comp. Methods Adv. Geomech. 3 (1994), 2151–2158.

[50] L. Shan, H. Zheng, and W. J. Layton, *A decoupling method with different subdomain time steps for the nonstationary Stokes–Darcy model*, Numer. Methods Partial Differ. Equ. 29 (2013), no. 2, 549–583.

[51] G. Singh, *Coupled flow and geomechanics modeling for fractured poroelastic reservoirs*, Ph.D. thesis, The University of Texas at Austin, 2014.

[52] J. C. Small, J. R. Booker, and E. H. Davis, *Elasto-plastic consolidation of soil*, Int. J. Solids Struct. 12 (1976), no. 6, 431–448.

[53] E. Storvik, J. W. Both, K. Kumar, J. M. Nordbotten, and F. A. Radu, *On the optimization of the fixed-stress splitting for Biot's equations*, Int. J. Numer. Methods Eng. 120 (2019), no. 2, 179–194.

[54] K. von Terzaghi, *Theoretical soil mechanics*, Wiley, New York, 1943.

[55] M. F. Wheeler, G. Xue, and I. Yotov, *A family of multipoint flux mixed finite element methods for elliptic problems on general grids*, Procedia Comput. Sci. 4 (2011), 918–927.

[56] M. F. Wheeler and I. Yotov, *A multipoint flux mixed finite element method*, SIAM J. Numer. Anal. 44 (2006), 2082–2106.

[57] J. A. White, N. Castelletto, and H. A. Tchelepi, *Block-partitioned solvers for coupled poromechanics: A unified framework*, Comput. Methods Appl. Mech. Eng. 303 (2016), 55–74.